

PREPARATION AND CHARACTERIZATION OF PHOTOCATALYST FOR THE CONVERSION OF CO₂ TO METHANOL

NUR SABRINA BINTI RAHMAT

**BACHELOR OF CHEMICAL ENGINEERING (PURE)
UNIVERSITI MALAYSIA PAHANG**

©NUR SABRINA BINTI RAHMAT (2015)

Thesis Access Form

No _____ Location _____

Author :

Title :

Status of access OPEN / RESTRICTED / CONFIDENTIAL

Moratorium period: _____ years, ending _____ / _____ 200 _____

Conditions of access proved by (CAPITALS): DR JOLIUS GIMBUN

Supervisor (Signature).....

Faculty:

Author's Declaration: *I agree the following conditions:*

OPEN access work shall be made available in the Universiti Malaysia Pahang only and not allowed to reproduce for any purposes.

The statement itself shall apply to ALL copies:

This copy has been supplied on the understanding that it is copyright material and that no quotation from the thesis may be published without proper acknowledgement.

Restricted/confidential work: All access and any photocopying shall be strictly subject to written permission from the University Head of Department and any external sponsor, if any.

Author's signature.....Date:

users declaration: for signature during any Moratorium period (Not Open work):

I undertake to uphold the above conditions:

Date	Name (CAPITALS)	Signature	Address

PREPARATION AND CHARACTERIZATION OF PHOTOCATALYST FOR THE CONVERSION OF CO₂ TO METHANOL

NUR SABRINA BINTI RAHMAT

Thesis submitted in partial fulfilment of the requirements
for the award of the degree of
Bachelor of Chemical Engineering (Pure)

**Faculty of Chemical & Natural Resources Engineering
UNIVERSITI MALAYSIA PAHANG**

JANUARY 2015

©NUR SABRINA BINTI RAHMAT (2015)

SUPERVISOR'S DECLARATION

We hereby declare that we have checked this thesis and in our opinion, this thesis is adequate in terms of scope and quality for the award of the degree of Bachelor of Chemical Engineering (Pure).

Signature	:
Name of main supervisor	: P. M. DR. MD MAKSUDUR RAHMAN KHAN
Position	: ASSOCIATE PROFESSOR
Date	: JANUARY 2015

STUDENT'S DECLARATION

I hereby declare that the work in this thesis is my own except for quotations and summaries which have been duly acknowledged. The thesis has not been accepted for any degree and is not concurrently submitted for award of other degree.

Signature :
Name : NUR SABRINA BINTI RAHMAT
ID Number : KA11050
Date : JANUARY 2015

Dedication

*To my beloved parents, family and friends.
Thank you for always being there for me.*

ACKNOWLEDGEMENT

Special thanks to Universiti Malaysia Pahang (UMP), that will soon become my alma mater, particularly Faculty of Chemical Engineering and Natural Resources that had given me the chance to complete my undergraduate research project for my bachelor degree. I am very pleased to recognize my supportive supervisor, P. M. Dr. Md Maksudur Rahman Khan who has contributed so much in helping me to complete my undergraduate research project. My gratification for his contribution can never be enough and this undergraduate research project would have not been completed successfully if it was not for his help and presence. Thank you.

I would like to express my gratitude to my personal advisor, Dr Syarifah Binti Abd Rahim who has advised and shared her insights with me throughout the whole years of my study in the university. Thank you for being patient and wise in dealing with some of the problems occurred during my study years.

A million thanks to both of my parents, Rahmat Bin Kader Baba and Mashuri Abu Bakar for their love, support and guidance as they help to build my spirit. They were the one who has supported me not only financially but with deep words for me to finish up my project until the end. Also not to forget my brother, Muhamad Anwar and sister, Nur Mimi Liyana who always has cheered me up and supported me in completing my project.

Finally, I would like to dedicate special thanks to my peer especially Vignes Rasiah and others for always being there for me and also to those who indirectly give moral support to me during the whole two semesters carrying out this undergraduate research project. May Allah SWT bless all of you. Thank you.

ABSTRACT

Due to the reliance of the world on fossil fuel as major source of energy, the CO₂ emission to the environment is inevitable which is responsible for global warming. Photocatalytic reduction of CO₂ to fuel, such as methanol, methane etc. is a promising way to address the CO₂ emission and energy crisis. The methanol produces from the photocatalytic conversion can be used as source of fuel. CdS is a classical photocatalyst shows high activity under ultraviolet (UV) light irradiation. UV light covers only 4% of the solar light spectrum, hence visible light active photocatalyst for CO₂ conversion is important. In the present work, Bi₂S₃/CdS was synthesized as an effective visible light responsive photocatalyst for CO₂ reduction. The Bi₂S₃/CdS photocatalyst was prepared by the hydrothermal reaction between the precursors. The prepared powder was calcined at 250 °C in the muffle furnace. The catalyst was characterized by X-ray diffraction (XRD) and Fourier Transform Infrared spectroscopy (FTIR). The product has been analysed by using gas chromatograph flame ionization detector (GC-FID). The photocatalytic activity in methanol production as a function of time has been investigated. The maximum yield of methanol was obtained after 6 hours of reaction. The effect of CdS concentration in Bi₂S₃/CdS photocatalyst was investigated and the yields of methanol were increased with increasing of CdS concentration. The maximum yield of methanol was obtained with Bi₂S₃/CdS with 45 % of CdS. The present works shown the potentially of Bi₂S₃/CdS for CO₂ reduction under visible light.

ABSTRAK

Kebergantungan dunia kepada bahan api fosil sebagai sumber utama tenaga telah menyebabkan pelepasan karbon dioksida kepada alam sekitar tidak dapat dielakkan dan berlakunya pemanasan global. Cara yang cemerlang untuk menangani krisis pelepasan karbon dioksida dan tenaga adalah dengan fotopemangkin pengurangan karbon dioksida Untuk mejana methanol metana dan lain-lain. Metanol yang dihasilkan dari penukaran photocataytic boleh digunakan sebagai sumber bahan api. CdS adalah fotomangkin klasik yang menunjukkan aktiviti yang tinggi di bawah sinaran ultraviolet (UV). Cahaya UV hanya meliputi 4% daripada spektrum cahaya matahari, justeu cahaya fotomangkin aktif untuk penukaran karbon dioksida adalah penting. Dalam kajian ini, $\text{Bi}_2\text{S}_3/\text{CdS}$ telah disintesis sebagai fotomangkin responsif cahaya yang boleh dilihat berkesan untuk pengurangan karbon dioksida. $\text{Bi}_2\text{S}_3/\text{CdS}$ fotomangkin telah disediakan oleh reaksi hidroterma antara prekursor. Serbuk telah dibakar pada $250\text{ }^{\circ}\text{C}$ dalam meredam relau. Pemangkin yang dicirikan oleh pembelauan sinar-X (XRD) dan Fourier Transform spektroskopi inframerah (FTIR). Produk reaksi ini telah dianalisis dengan menggunakan alat kromatografi gas pengesan pengionan nyala (GC-FID). Aktiviti fotopemangkinan dalam pengeluaran metanol sebagai fungsi masa telah disiasat. Hasil maksimum metanol telah diperolehi selepas 6 jam tindak balas. Kesan kepekatan CdS dalam $\text{Bi}_2\text{S}_3/\text{CdS}$ fotomangkin telah disiasat dan hasil metanol telah meningkat dengan peningkatan kepekatan CdS. Hasil maksimum metanol telah diperolehi dengan $\text{Bi}_2\text{S}_3/\text{CdS}$ dengan 45% daripada CdS. Kerja-kerja ini ditunjukkan yang berpotensi daripada $\text{Bi}_2\text{S}_3/\text{CdS}$ untuk pengurangan karbon dioksida di bawah cahaya yang boleh dilihat.

TABLE OF CONTENTS

SUPERVISOR'S DECLARATION	IV
STUDENT'S DECLARATION	V
<i>Dedication</i>	VI
ACKNOWLEDGEMENT	VII
ABSTRACT.....	VIII
ABSTRAK.....	IX
TABLE OF CONTENTS.....	X
LIST OF FIGURES	XI
1 INTRODUCTION	1
1.1 Motivation and statement of problem	1
1.2 Objectives.....	2
1.3 Scope of this research.....	2
2 LITERATURE REVIEW	3
2.1 Overview	3
2.2 Fundamentals in photocatalysis	3
2.3 Decomposition of water, H ₂ O	6
2.4 Selection of Bi ₂ S ₃ /CdS as the catalyst	8
2.5 Summary	10
3 MATERIALS AND METHODS.....	11
3.1 Chemicals.....	11
3.2 Preparation of photocatalysts	11
3.3 Characterization	11
3.4 Photocatalytic experiment.....	12
4 RESULTS AND DISCUSSION	14
4.1 The presence of methanol	14
4.2 UV-Vis spectroscopy analysis	16
4.3 X-ray Diffraction (XRD) analysis.....	18
4.4 Fourier Transform Infrared Spectroscopy (FTIR) analysis	21
4.5 Photocatalytic activity	23
5 CONCLUSION AND RECOMMENDATIONS	25
5.1 Conclusion.....	25
5.2 Recommendations	25
REFERENCES	26
APPENDIXES	28
APPENDIX A.1	28
A.1.1 Chemicals.....	28
A.1.2 Experiments	30
A.1.3 Catalysts produced	34
A.1.4 Products produced.....	35
A.1.5 XRD Analysis	41
A.1.6 FTIR Analysis (Solid).....	45
A.1.7 FTIR Analysis (Liquid).....	47
A.1.8 GC-FID	49

LIST OF FIGURES

Figure 2-1 Schematic representation of band gap formation and photocatalytic processes (Muhammad Tahir et al., 2013)	4
Figure 2-2 Mechanism and pathways for photocatalytic oxidation and reduction processes on the surface of heterogeneous photocatalyst. (Muhammad Tahir et al., 2013)	5
Figure 2-3 Illustration of the decomposition and splitting of water, H_2O	7
Figure 2-4 Illustration of the bandgap of semiconductors in photocatalytic	9
Figure 3-1 Illustration on how the experiment were done	13
Figure 4-1 The sample from the experiment	14
Figure 4-2 The pure methanol, the sample and the Jones oxidation reagent.....	15
Figure 4-3 The pure methanol, the sample and the Jones oxidation reagent after diluted with water to run in UV-Vis spectrometer.....	15
Figure 4-4 (a) & (b) Pure methanol detection by UV-Vis	16
Figure 4-5 (a) & (b) Methanol detection in a sample by UV-Vis.....	17
Figure 4-6 XRD pattern of CdS shown as a reference	19
Figure 4-7 FTIR patterns of various photocatalysts	21
Figure 4-8 FTIR patterns from the photocatalytic reaction testing	22
Figure 4-10 The yields of CH_3OH in the photocatalytic reduction of CO_2 with H_2O over various photocatalysts under visible light irradiation	23
Figure 4-11 The mechanism of photocatalytic reduction for production of CH_3OH	24

1 INTRODUCTION

1.1 Motivation and statement of problem

Sustainable development depends directly on the availability of sufficient energy resources, consumption over restoration ratios and effects of energy on the environment (Ghoniem AF., 2011). Consequently, rapid industrialization and modernization has amplified energy demands while fossil fuels have remained as the main source of energy, exacerbating critical social issues like security of energy supply and climate change (Gill SS et al., 2010).

Threats of global warming and energy crisis had accelerated the rush for new renewable energy resources. In order to reduce carbon dioxide emission and to produce a maintainable fuels, recycling the greenhouse gases such as carbon dioxide seems eminently potential. Due to the increasing levels of carbon dioxide emissions from fossil fuels consumption, the problem of global warming has aroused into public concern (C. Song, 2006). One of the biggest challenges are to seek a renewable energy which not only meet the increasing energy demand, but also to replace the traditional chemicals fuels and environmentally friendly. One of the prospective way to reuse hydrocarbon resources is the photocatalytic reduction of CO_2 with H_2O utilizing the solar energy (S.C. Roy et al., 2010). By using this way, carbon dioxide emissions can be reduced and energy crisis can be solved.

The most popular photocatalytic material with excellent stability, innocuity and low price (H.-C. Yang et al., 2009), three-dimensional, larger surface and regular structure (G.K. Mor et al., 2006) is titanium dioxide (TiO_2). Differ from the massive or grainy semiconductor materials, TiO_2 structures show typically a super hydrophilic behaviour (J.M. Macak et al., 2007) and quickly transfer electron (K. Zhu et al., 2007). However, TiO_2 have a low quantum efficiency, which increase the combining ratio of electrons and holes. It can only absorb 5% sunlight in the ultraviolet region since it is a wide band gap semiconductor (3.0-3.2 eV) (M. Hoffmann et al., 1995). It is well known that the band gaps of CdS and Bi_2S_3 are narrower and the potentials of conduction bands are more negative compare to other photocatalysts (Vogel R et al., 1994).

The ideal photocatalyst having a gap of 1.5 eV is well approximated by narrow band gap semiconductor material and highly stable electrodes may be produced by appropriate surface modification in order to enhance the photocatalytic activity and visible light response.

1.2 Objectives

The following are the objectives of this research:

- To prepare, modify and characterize Bi₂S₃/CdS photocatalysts.
- To use the obtained Bi₂S₃/CdS as a photocatalyst for the photocatalytic reduction of carbon dioxide to methanol with water under visible light radiation

1.3 Scope of this research

The following are the scope of this research:

- The CdS was modified by Bi₂S₃ and the obtained Bi₂S₃/CdS were used as a photocatalyst for the photocatalytic reduction of carbon dioxide to methanol with water under visible light radiation.
- The Bi₂S₃, CdS and Bi₂S₃/CdS photocatalysts were characterized by X-ray diffraction (XRD) and Fourier transform infrared spectroscopy (FTIR).
- The photocatalytic activities of the Bi₂S₃, CdS and Bi₂S₃/CdS photocatalysts for reducing carbon dioxide, CO₂ to methanol, CH₃OH under visible light irradiation were investigated by Fourier transform infrared spectroscopy (FTIR) and gas chromatography/flame ionization detection (GC/FID).

2 LITERATURE REVIEW

2.1 Overview

This paper presents about the CdS and Bi₂S₃ which are synthesized into a new type of heterostructure photocatalyst which lower the photocatalytic efficiency of TiO₂ under visible light irradiation by decomposing the water, H₂O to produce methanol as the a reusable hydrocarbon.

2.2 Fundamentals in photocatalysis

Photocatalysis is a process in which light radiation having energy equal to or greater than the band gap energy (E_{bg}) of a semiconductor strikes on its surface and generates electron (e⁻) hole and (h⁺) pairs. The photogenerated electrons and holes participate in various oxidation and reduction processes to produce final products. However, if the charges fail to find any trapped species on the surface or their energy band gap is too small, they recombine immediately releasing unproductive energy as heat (Kavita K, et al., 2004). In particular, the activity of heterogeneous photocatalysis depends on :

- (a) composition of reaction medium
- (b) adsorption of reactants on semiconductor surface
- (c) type of semiconductor and its crystallographic or morphological characteristics
- (d) ability of semiconductor to absorb UV (ultraviolet) or visible light (Hd Lasa et al, 2005)

During photoreduction process, several processes related to catalyst, interface and donor-acceptor are involved as explained in Figure 2.1. In catalyst related process, there is production of electrons and holes by absorbing photons. The lifetime of the charges is few nanoseconds only, therefore several recombine immediately and others participate in carrying various chemical reactions. Interface related process consists of transfer of electrons and adsorption on catalyst surface and mass transfer. In donor-acceptor related process, electrons and holes which escape from the excitation regions are trapped by adsorbed species, which become active and participate in various reduction and oxidation process.

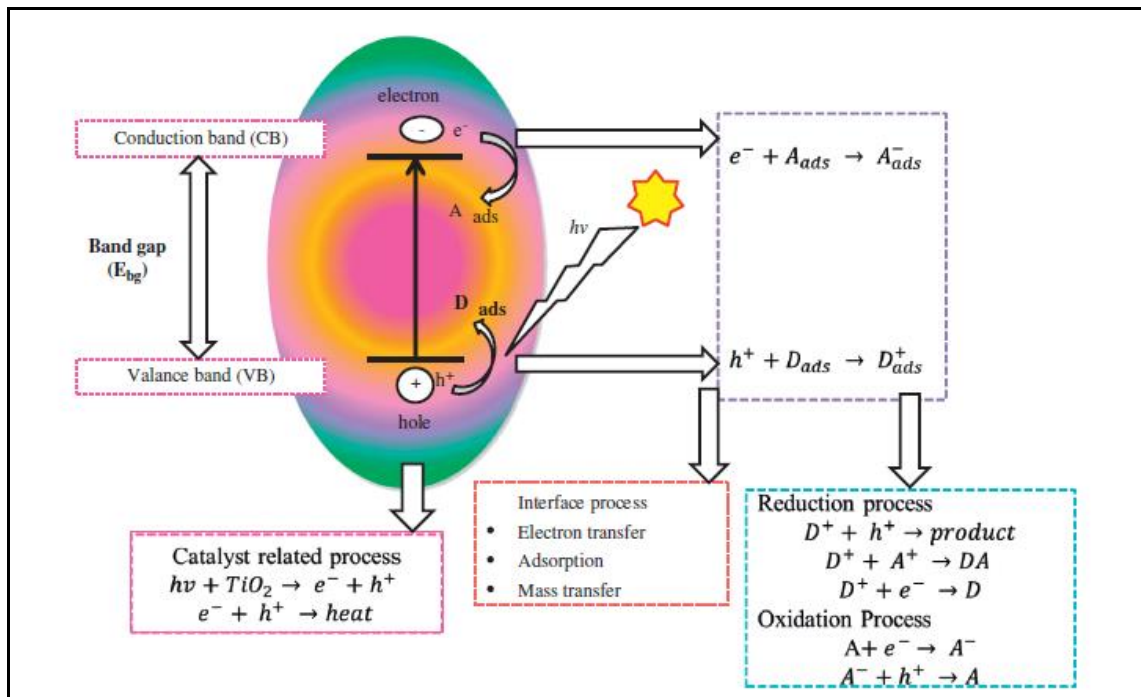


Figure 2-1 Schematic representation of band gap formation and photocatalytic processes (Muhammad Tahir et al., 2013)

Detailed explanation of photoreduction surface phenomenon for heterogeneous photocatalysis is presented in Figure 2.2. The heterogeneous photocatalysis mechanism is very complex and many possibilities or reaction paths are possible. This depends on the life of charge particles if their energy band gap is lower and recombines immediately.

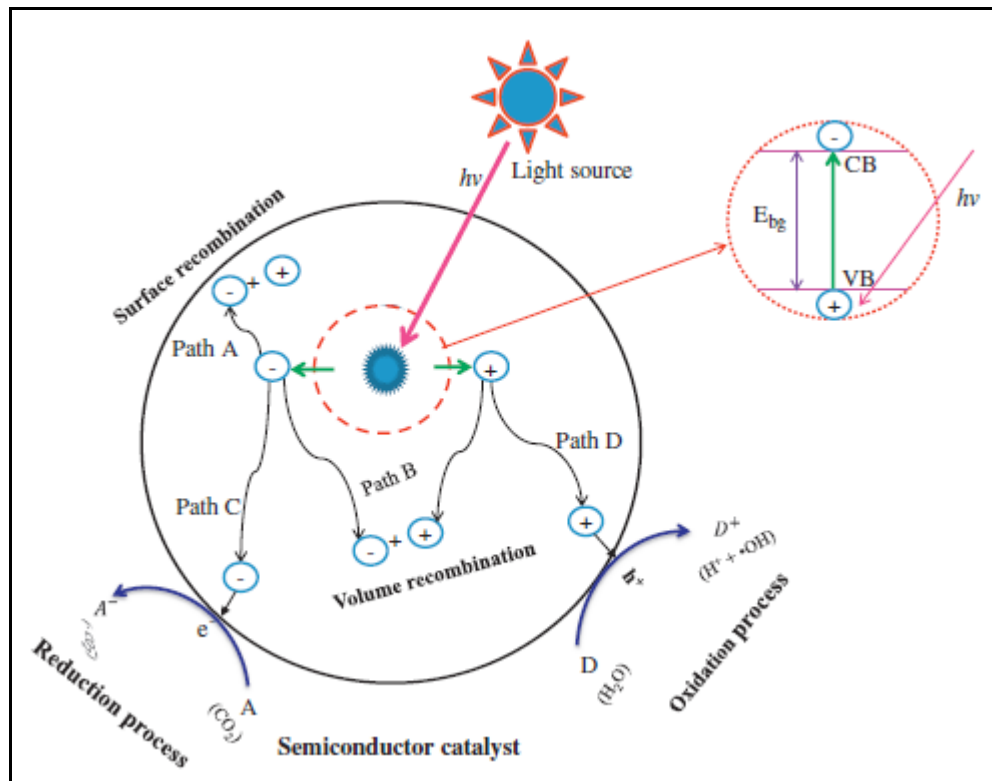


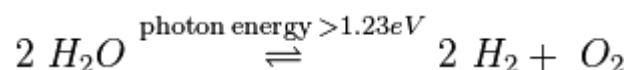
Figure 2-2 Mechanism and pathways for photocatalytic oxidation and reduction processes on the surface of heterogeneous photocatalyst. (Muhammad Tahir et al., 2013)

However, if the charge particles have enough band gap energies to separate, then the following possibilities or paths are possible (Arakawa H et al., 2001) :

- a) The photoinduced charges move towards the surface of semiconductor and transfer electrons or holes to adsorbed species. The electron transfer process is more effective if pre-adsorbed species already exist at the surface. At the surface, semiconductor can donate electron to reduce acceptors (Path C), in turn a hole can transfer to the surface where an electron from donor species can combine with the surface hole, oxidizing donor species (Path D).
- b) During charges transfer process, there is possibility of electron–hole recombination. Recombination of separated electron and holes can possible in the volume or at the surface of semiconductor with the release of unproductive heat.
- c) Surface recombination (Path A) occurred when electrons and holes recombine on the semiconductor surface. On the other hand, if charges have the opportunity to recombine inside the semiconductor volume, then this process is called volume recombination (Path B).

2.3 Decomposition of water, H_2O

The photocatalytic reduction of CO_2 with H_2O to reusable hydrocarbon resources such as methanol is found to be a prospective way to reduce carbon dioxide emissions and resolve the energy crisis. The catalyst is use to split the H_2O . When H_2O decompose and split into O_2 and H_2 , the stoichiometric ratio of its products is 2:1 :



The process of water-splitting is a highly endothermic process ($\Delta H > 0$). The minimum potential difference (voltage) needed to split water is 1.23V at 0 pH (J. Head, J. Turner, 2001). Since the minimum band gap for successful water splitting at pH=0 is 1.23 eV, corresponding to light of 1008 nm, the electrochemical requirements can theoretically reach down into infrared light, albeit with negligible catalytic activity. These values are true only for a completely reversible reaction at standard temperature and pressure (1 bar and 25 °C).

The potential must be less than 3.0V to make efficient use of the energy present across the full spectrum of sunlight. Water splitting can transfer charges, but not be able to avoid corrosion for long term stability. Defects within crystalline photocatalysts can act as recombination sites, ultimately lowering efficiency.

Materials used in photocatalytic water splitting fulfill the band requirements outlined previously and typically have dopants and/or co-catalysts added to optimize their performance.

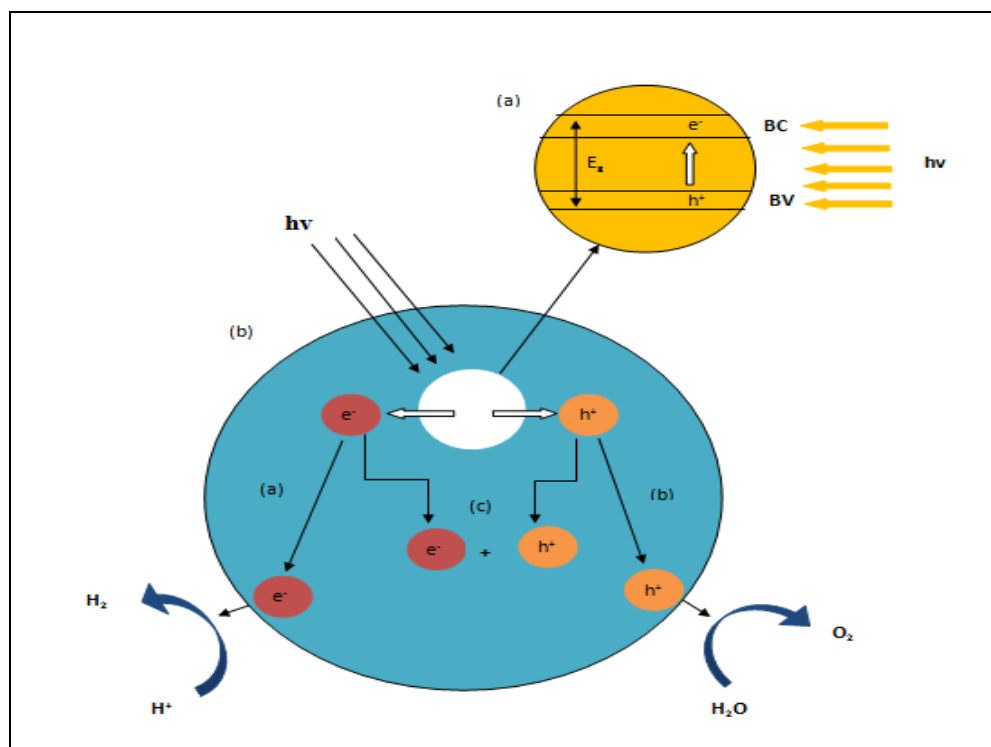


Figure 2-3 Illustration of the decomposition and splitting of water, H₂O

2.4 Selection of $\text{Bi}_2\text{S}_3/\text{CdS}$ as the catalyst

The effectiveness of semiconductors to transfer photo-induced electron toward adsorbed species depends on the semiconductor conductance band and redox potential of adsorbates. The band gap of semiconductor indicates its ability to absorb photons. Usually large band gap materials are most suitable for CO_2 reduction applications as they can provide enough redox potentials to execute chemical reaction. However, large band gaps require higher input energy (Linsebigler A L et al, 1995).

The limitation of photocatalytic activity for semiconductors can also be overcome by surface modification. Semiconductor surface modification has three advantages :

- (a) inhibiting recombination by increasing charge separation which ultimately increases efficiency
- (b) enhancing wavelength response
- (c) increasing selectivity or yield of desired product

The design of molecular size catalysts within zeolite and other porous materials having micro pores is of special interest due to distinct physical and chemical properties (Mori K et al., 2012). Micro structured materials have many advantages including higher internal surface area, ion exchange capacities and porous structure allowing the molecules to diffuse in to pores cavities and remain intact during cluster growth (Anpo M, 1995). Different types of sensitizers such as coupling semiconductors, carbon nanotubes, and some novel sensitizers could also be used to improve photocatalytic activity and selectivity under solar spectrum.

It is well known that the band gaps of CdS and Bi_2S_3 are narrower and the potentials of conduction bands are more negative compare to other photocatalysts. The CdS and Bi_2S_3 have higher quantum efficiency, which decrease the combining ratio of electrons and holes. It can also absorb more than 5% sunlight in the ultraviolet since it is a narrow band gap semiconductor.

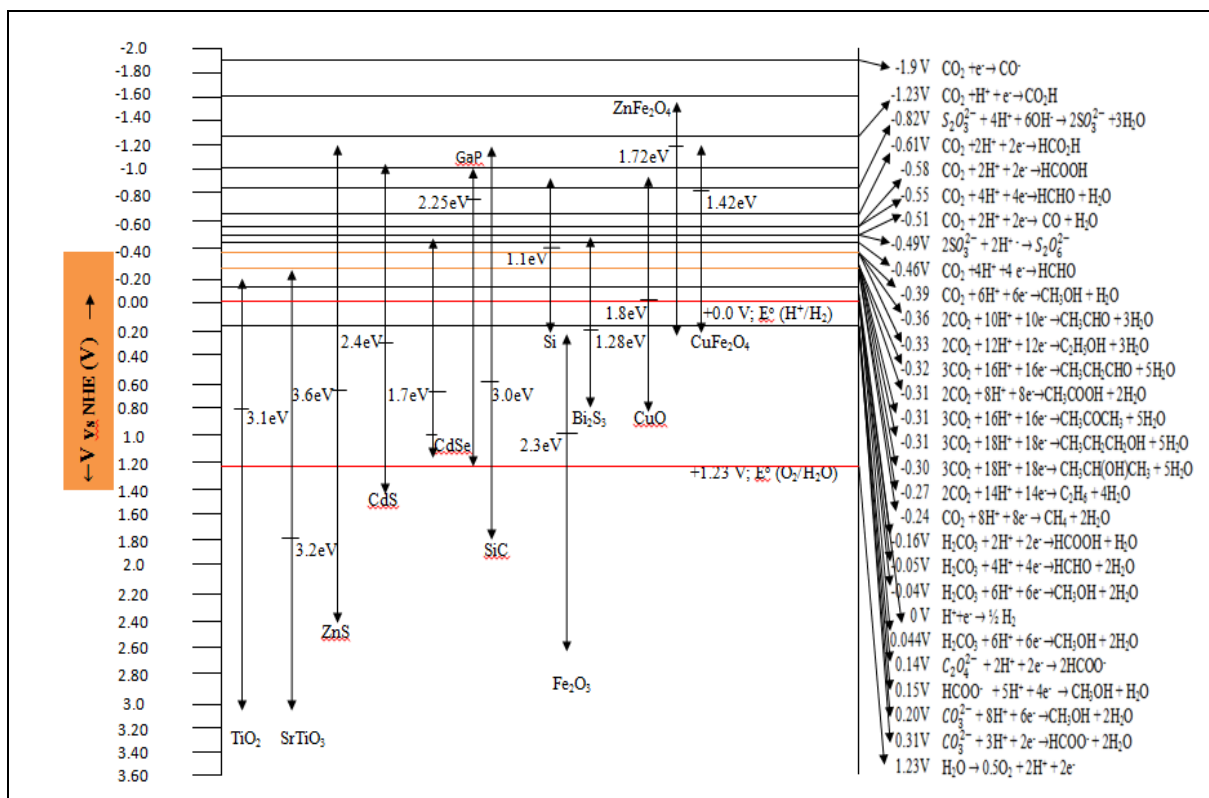


Figure 2-4 Illustration of the bandgap of semiconductors in photocatalytic

In 1979, Inoue et al. first reported that CO_2 bubbled in water was reduced to HCHO, HCOOH and CH_3OH over various semiconductor photocatalysts, such as CdS, TiO_2 , ZnO, GaP and SiC under photoirradiation of their aqueous suspension. Aliwi and Al-Jubori carried out the photoreduction of CO_2 in the presence of H_2S over typical sulfides such as bismuth sulfide (Bi_2S_3) and cadmium sulfide (CdS). HCHO and HCOOH were produced in this reaction.

The photocatalytic reduction of CO_2 over hexagonal CdS nanocrystallites prepared in N, N-dimethylformamide (DMF) was investigated by Fujiwara and his co-workers and they found that sulfur vacancies on the surface of nanocrystallites can be formed by the adsorption of excess Cd^{2+} to the surface, which resulted in a remarkable increase of photocatalytic activity. Eggins and his co-workers performed the photocatalytic reduction of CO_2 to dimeric and tetrameric products, namely oxalate, glyoxylate, glycolate and tartrate using aqueous CdS or ZnS colloids containing tetramethylammonium chloride.

2.5 Summary

This paper presents about the CdS and Bi₂S₃ can be utilized as sensitizers and applied to synthesize a new type of heterostructure photocatalyst which can solve the instability of sulphides and lower the photocatalytic efficiency of TiO₂ under visible light irradiation. A better photoabsorption performance can be determined from the yield of methanol with the photocatalytic activity of Bi₂S₃/CdS.

3 MATERIALS AND METHODS

3.1 Chemicals

The chemical reagents used in this experiment were thio-urea, cadmium nitrate tetrahydrate, cadmium sulfide (CdS) powder, bismuth III nitrate pentahydrate, sodium nitrite, potassium hydroxide and sodium sulphite. All chemicals were ~99% purity obtained from Sigma, USA.

3.2 Preparation of photocatalysts

The Bi₂S₃/CdS catalyst was prepared by following direct hydrothermal method. Cd(NO₃)₂·4H₂O, Bi(NO₃)₃·5H₂O and thio-urea of different compositions such as 6.02, 3.05 and 2.26 g, respectively were considered for the preparation followed by hydrolysis with 600 mL of deionized water in an autoclave at 90-100°C for 6 h. Then cooled down to room temperature and successively the precipitate was filtered off, washed with distilled water and dried in an oven at 60°C overnight. The catalyst was grinded with mortar before calcined at 250°C for 3 h. Similarly, the weight proportions of Bi₂S₃ to CdS were 15% Bi₂S₃/CdS, 30% Bi₂S₃/CdS and 45% Bi₂S₃/CdS were prepared with the same method.

3.3 Characterization

The X-ray diffraction (XRD) patterns were obtained at room temperature using MSAL-XD2 diffractometer with Cu K_α radiation (operated at 36 kV and 30 mA, $\lambda = 0.15406$ nm). The Fourier transform infrared spectroscopy (FTIR) patterns were also obtained for both sample and products.

3.4 Photocatalytic experiment

The photocatalytic experiment was performed in a photochemical reactor equipped with a magnetic stirrer, a quartz cool trap and a condensation tube. A 500 W Xe lamp was located in the quartz cool trap as illuminant. The UV light was removed by 1.0 M sodium nitrite solution. Sodium nitrite, potassium hydroxide and sodium sulphite of corresponding quantities 20.701, 1.225 and 3.789 g were dissolved in 300 mL of ultrafiltered water. The solution was then put into the photochemical reactor. Ultrapure CO₂ was bubbled through the solution in the reactor before irradiation for 30 min to ensure that all dissolved oxygen was eliminated. 0.2 g of catalyst powder was added into the solution and the irradiation lamp was turned on to start the photoreaction. The temperature with the range of 30-35°C was observed for every 1 h to avoid the loss of methanol into the air. Ultrapure CO₂ was continuously bubbled through the solution during the whole irradiation for 6 h. A needle-type probe was inserted into the solution of the reactor with the aid of vacuum pump to withdraw a small amount of liquid samples for 1 h interval up to 6 h. The concentrations of methanol in the samples were analysed using a gas chromatograph flame ionization detector (GC-FID).

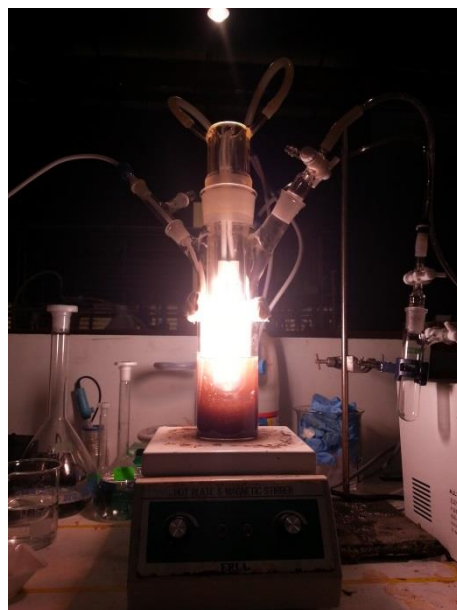
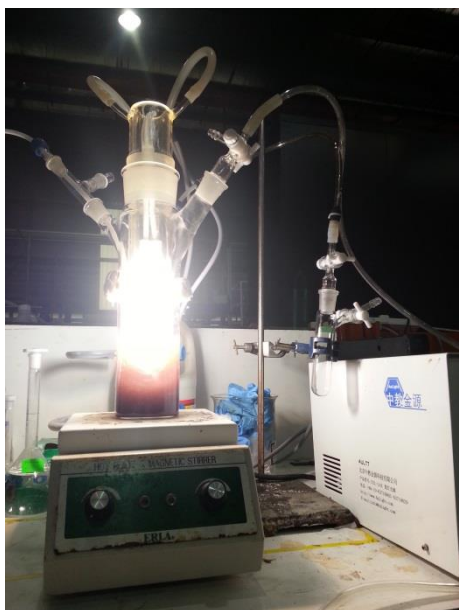
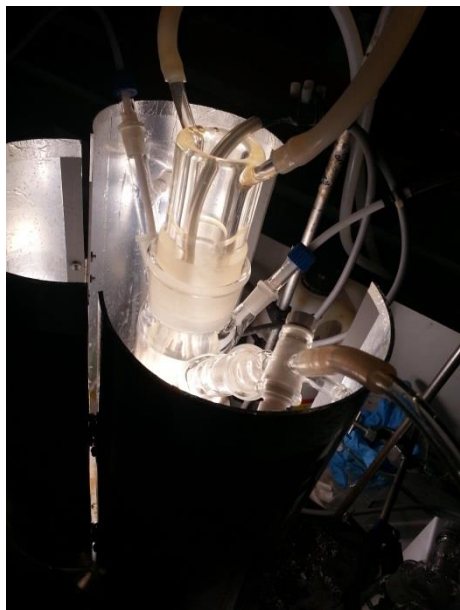
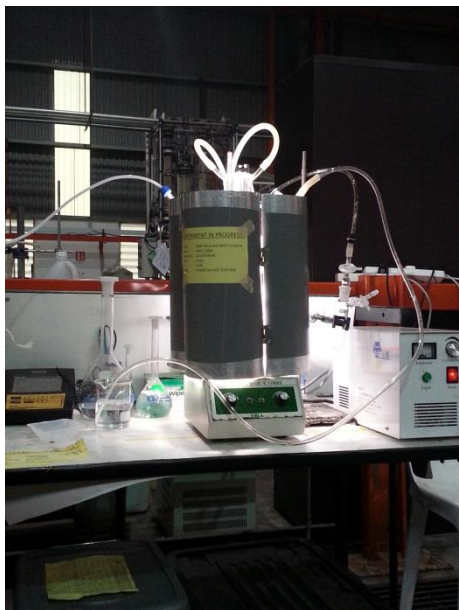


Figure 3-1 Illustration on how the experiment were done

4 RESULTS AND DISCUSSION

4.1 *The presence of methanol*

1. In a test tube, 1 ml of acetone + 3 drops of Jones oxidation reagent were added.
2. In a test tube, 1 ml of acetone + 200 μL of pure methanol + 3 drops of Jones oxidation reagent were added.
3. In a test tube, 1 ml of acetone + 200 μL of sample + 3 drops of Jones oxidation reagent were added.
4. For the calibration procedure and UV method, 250 μL solution and 2.5 ml of distilled water, each from the test tubes were put in cuvettes and the UV was run.



Figure 4-1 The sample from the experiment

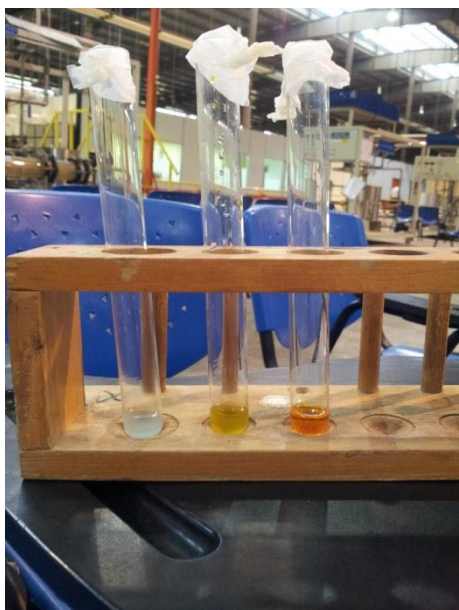


Figure 4-2 The pure methanol, the sample and the Jones oxidation reagent

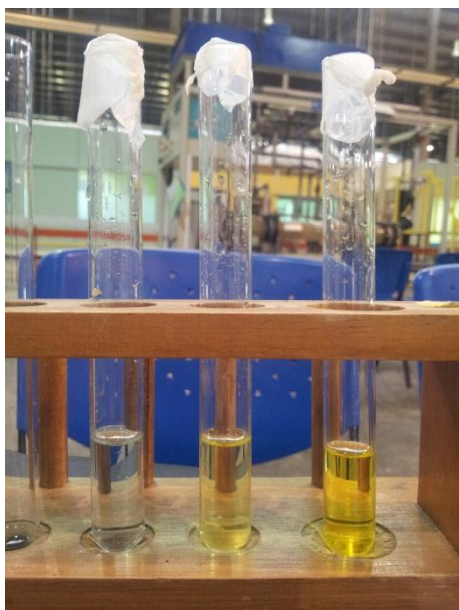
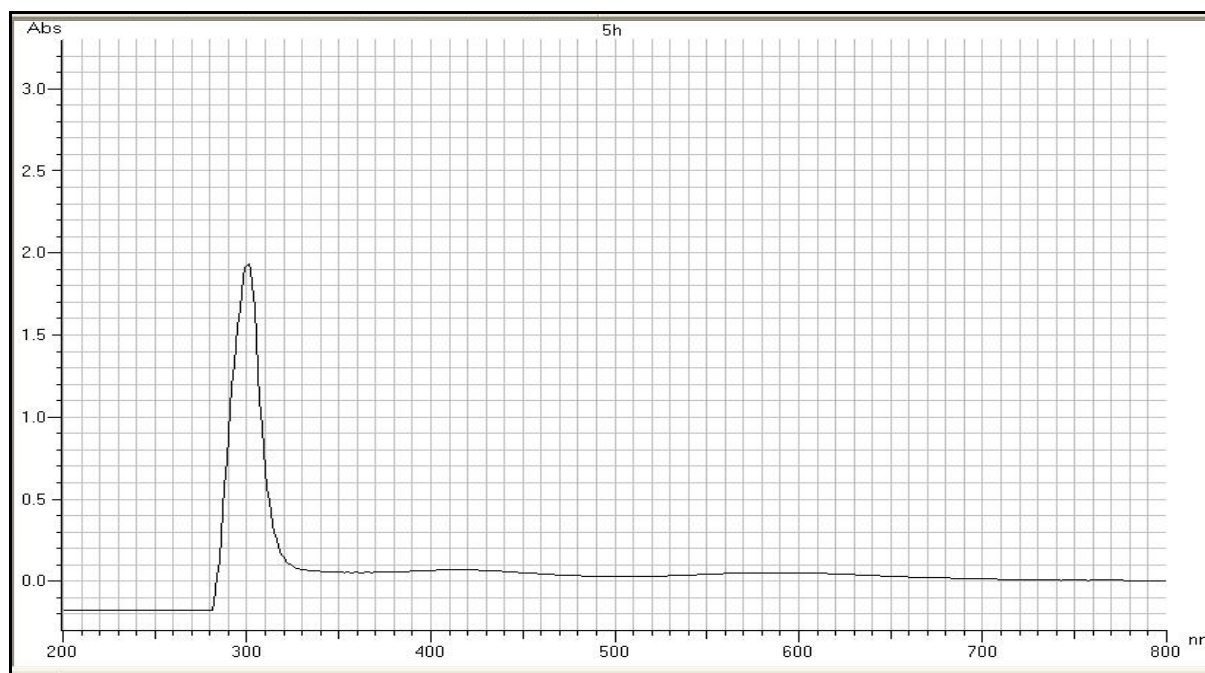


Figure 4-3 The pure methanol, the sample and the Jones oxidation reagent after diluted with water to run in UV-Vis spectrometer

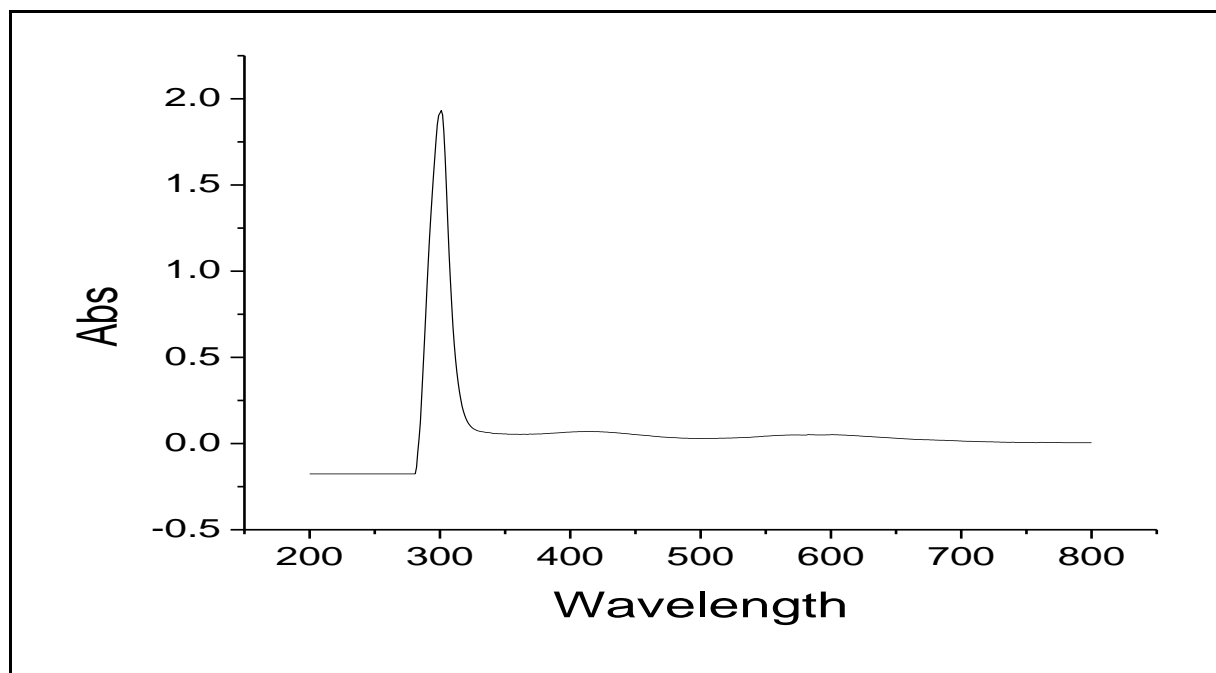
4.2 UV-Vis spectroscopy analysis

The UV-Vis spectra in the range of 200-800 nm was measured with a Daojin UV-2550PC diffuse reflectance spectroscope.

The results are as below :

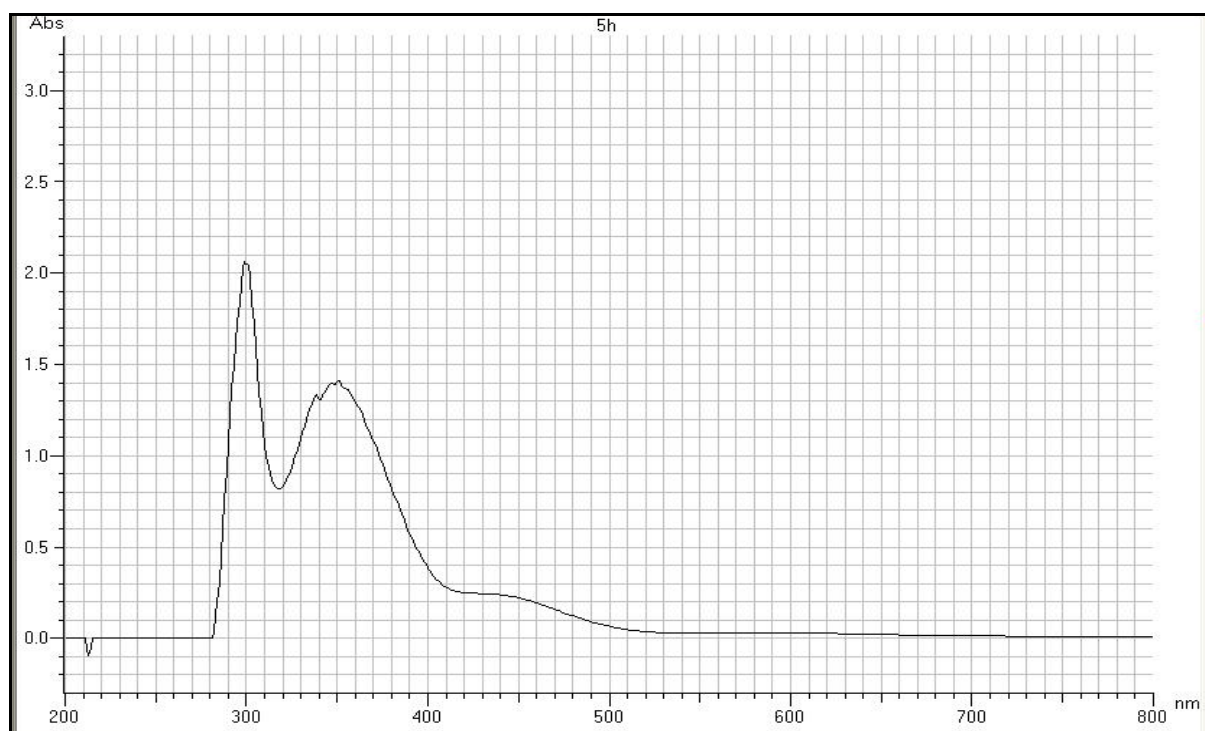


(a)

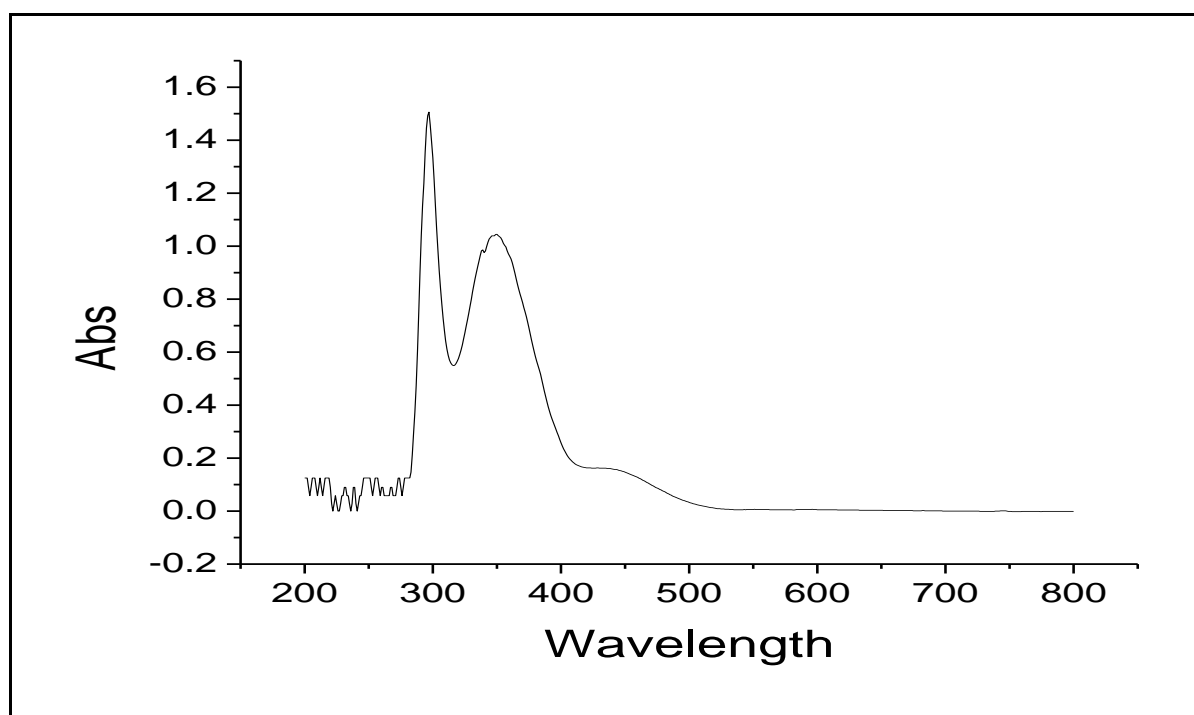


(b)

Figure 4-4 (a) & (b) Pure methanol detection by UV-Vis



(a)



(b)

Figure 4-5 (a) & (b) Methanol detection in a sample by UV-Vis

4.3 X-ray Diffraction (XRD) analysis

The XRD pattern of pure CdS is shown in the Figure 4.6 ($2\theta=3-80^\circ$), was used as a reference for the structural analysis of as-prepared $\text{Bi}_2\text{S}_3/\text{CdS}$ photocatalysts. XRD patterns of various as-prepared photocatalysts are shown in Figure 2(1-d) corresponding to (a) $\text{Bi}_2\text{S}_3/\text{CdS}$ (b) $\text{Bi}_2\text{S}_3/\text{CdS}$ (15%) (c) $\text{Bi}_2\text{S}_3/\text{CdS}$ (30%) (d) $\text{Bi}_2\text{S}_3/\text{CdS}$ (45%). The XRD patterns of the catalysts were recorded in the range of diffracting angles of $2\theta=3-80^\circ$ but shown only $2\theta=15-50^\circ$, the most significant portion. The XRD study reveals that CdS (15-45 wt%) incorporation in Bi_2S_3 takes place and gradual changes in the crystallographic parameters are detected. It was observed from the XRD analysis that there are mainly two types of crystallite structures e.g., orthorhombic Bi_2S_3 and cubic CdS. Using Scherrer formula for the full width at half maximum (FWHM) of the main peaks, the average crystallite size of the CdS and Bi_2S_3 were found to be 5-30 nm and 30-50 nm, respectively. It has been noticed that the crystallite size of Bi_2S_3 increased with CdS loading. According to the standard diffraction peaks of cubic CdS (JCPDS # 89-0440), the sharp peaks were consistent with the peak positions of CdS (100, 002, 101) (Figure 4.6).

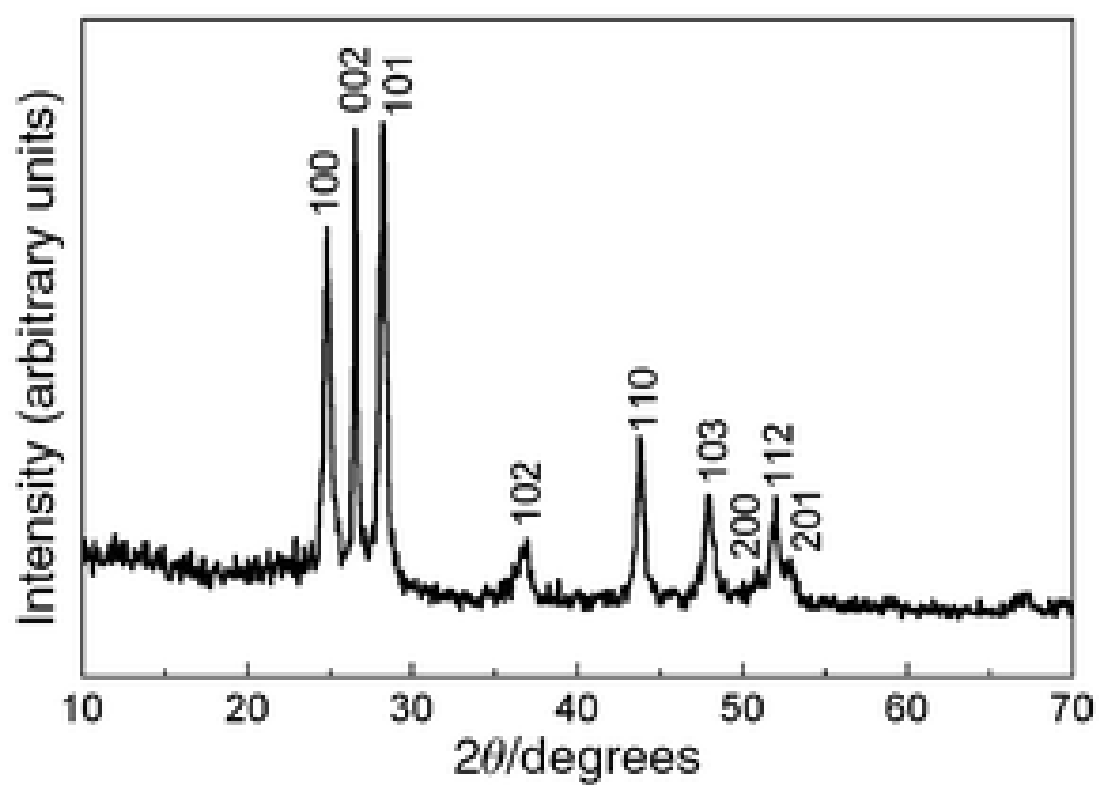


Figure 4-6 XRD pattern of CdS shown as a reference

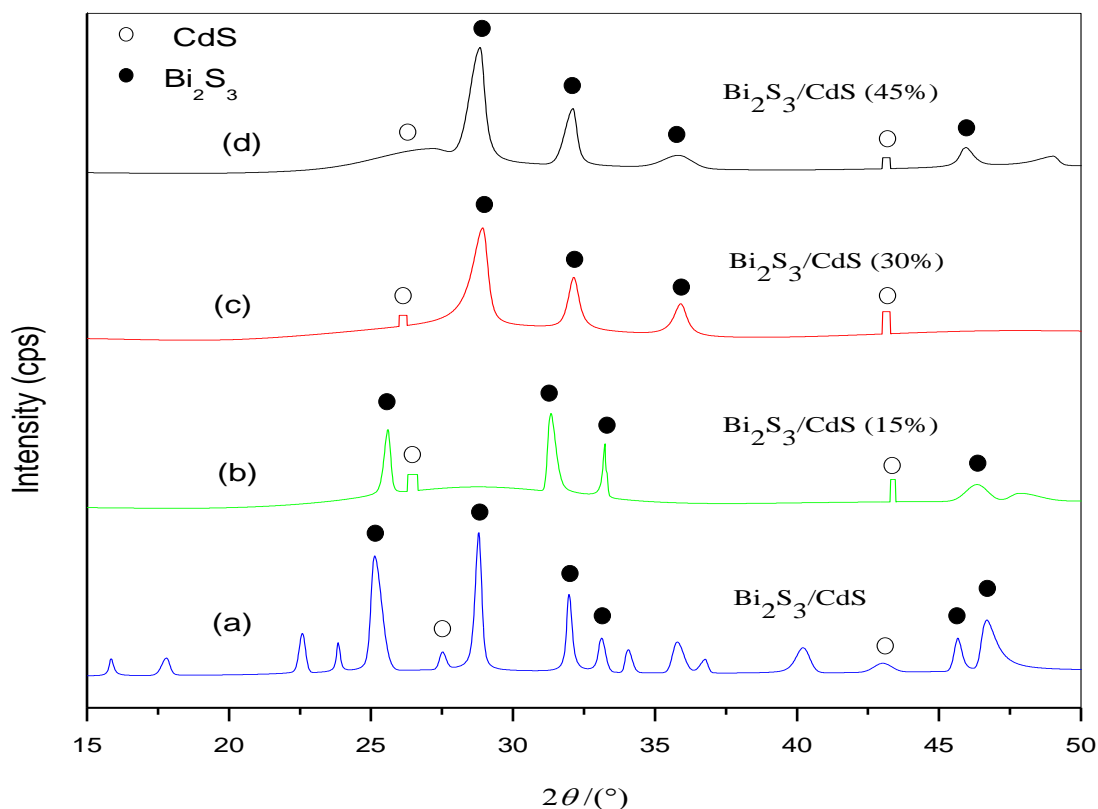


Figure 4-7 XRD patterns of various photocatalysts (a) $\text{Bi}_2\text{S}_3/\text{CdS}$ (b) $\text{Bi}_2\text{S}_3/\text{CdS}$ (15%) (c) $\text{Bi}_2\text{S}_3/\text{CdS}$ (30%) (d) $\text{Bi}_2\text{S}_3/\text{CdS}$ (45%)

It can be seen from the XRD spectrum of the Bi_2S_3 in Figure 4.7 that the peaks were in good agreement with the standard diffraction peaks of orthorhombic Bi_2S_3 (JCPDS # 17-0320). Five peaks with 2θ values of 25.1° , 28.78° , 31.94° , 46.62° and 53.72° in $\text{Bi}_2\text{S}_3/\text{CdS}$ correspond to the crystal planes of (130), (211), (221), (351) and (431) of orthorhombic phase Bi_2S_3 , respectively. The lattice parameters are estimated for orthorhombic structure of Bi_2S_3 and found to be $a_0=10.84 \text{ \AA}$ (standard $a_0=11.49 \text{ \AA}$), $b_0=11.38 \text{ \AA}$ (standard $b_0=11.30 \text{ \AA}$) and $c_0=3.97 \text{ \AA}$ (standard $c_0=3.981 \text{ \AA}$). Hence, it is confirmed that the Bi_2S_3 structure is orthorhombic.

Moreover, the peaks of all the $\text{Bi}_2\text{S}_3/\text{CdS}$ photocatalysts in Figure 4.7 suggesting that all the $\text{Bi}_2\text{S}_3/\text{CdS}$ photocatalysts are all composed of the two crystallite phases and there are no unknown phases proved that they do not react with each other and make a hetero junction to show catalytic activities.

4.4 Fourier Transform Infrared Spectroscopy (FTIR) analysis

FTIR was carried out to identify the component and chemical compositions which exist in the $\text{Bi}_2\text{S}_3/\text{CdS}$ photocatalysts and the product which is methanol from the photocatalytic reaction testing. From Figure 4.8, it can be seen that from FTIR spectra of adsorbed $\text{Bi}_2\text{S}_3/\text{CdS}$ are from $500 - 2000 \text{ cm}^{-1}$ while photocatalysts of $\text{Bi}_2\text{S}_3/\text{CdS}$ (15%), $\text{Bi}_2\text{S}_3/\text{CdS}$ (30%) and $\text{Bi}_2\text{S}_3/\text{CdS}$ (45%) are adsorbed from $500 - 700 \text{ cm}^{-1}$.

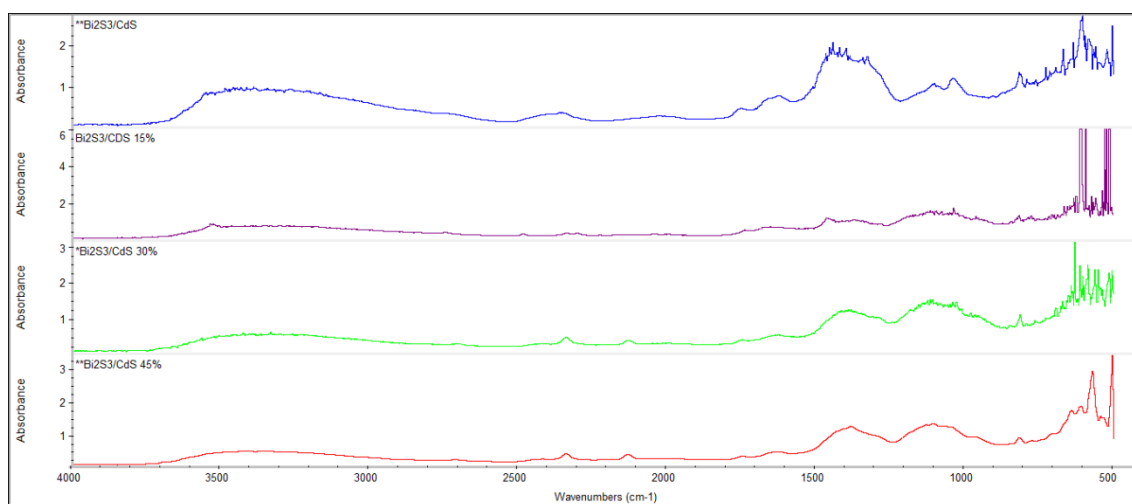


Figure 4-8 FTIR patterns of various photocatalysts

From Figure 4.9, it can be seen that from FTIR spectra of adsorbed methanol at room temperature of 298 K, formation of several absorption bands in the wavenumber region at $3000 - 3600 \text{ cm}^{-1}$ and above 1400 cm^{-1} . The intensity of absorption bands decreased after evacuation. Positions of these bands are very close to those of gaseous methanol. They can be attributed to undissociated methanol, which is weakly bound via H-bond on a cation-anion couple with basic character.

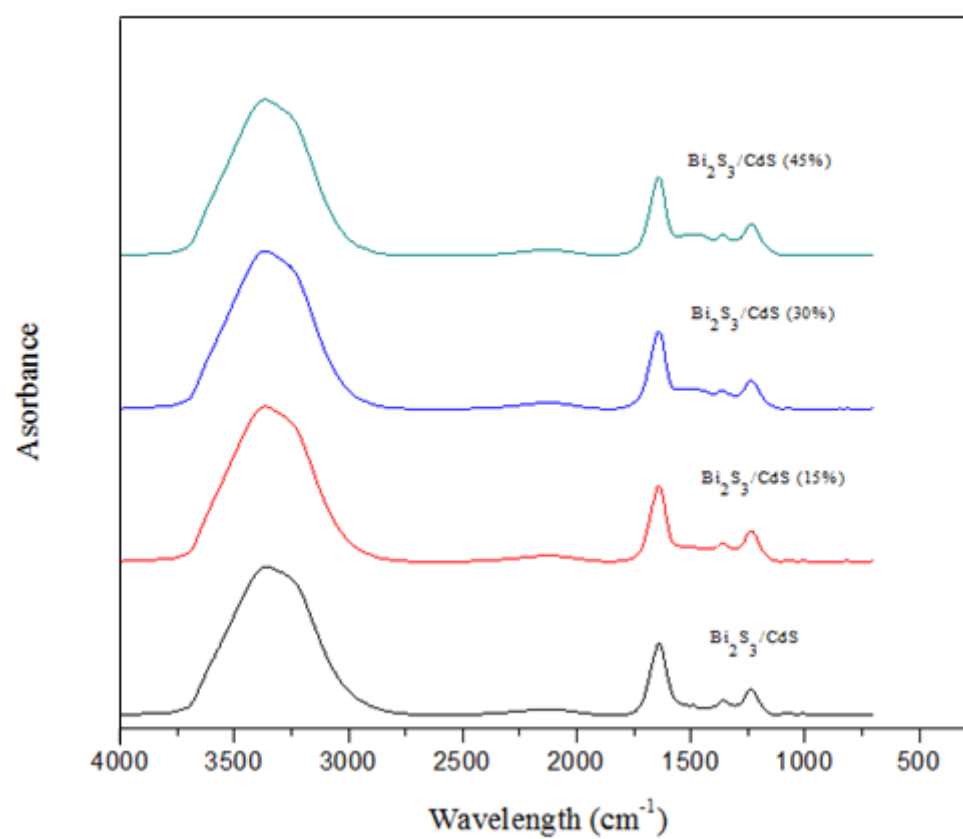


Figure 4-9 FTIR patterns from the photocatalytic reaction testing

4.5 Photocatalytic activity

The yields of CH_3OH in the photocatalytic reduction of CO_2 with H_2O on various photocatalysts under visible light irradiation are shown in Figure 4.10. From the figure, it can be seen that the generation rates of CH_3OH over the $\text{Bi}_2\text{S}_3/\text{CdS}$ were significantly higher when the concentration of CdS was increased. The highest yield of methanol over $\text{Bi}_2\text{S}_3/\text{CdS}$ was $20.04 \mu\text{mole/g}$ when the weight proportions of Bi_2S_3 to CdS were 45%. This may be due to doping Bi_2S_3 to CdS could form hetero-junction structures which improves the separation of electrons and holes, prevents the charge-carrier recombination and prolongs the lifetime of photo-carriers in $\text{Bi}_2\text{S}_3/\text{CdS}$ photocatalyst. In addition, the spread of belt-shaped Bi_2S_3 on the surface of CdS particles was better when the weight proportion of Bi_2S_3 to CdS was 45%.

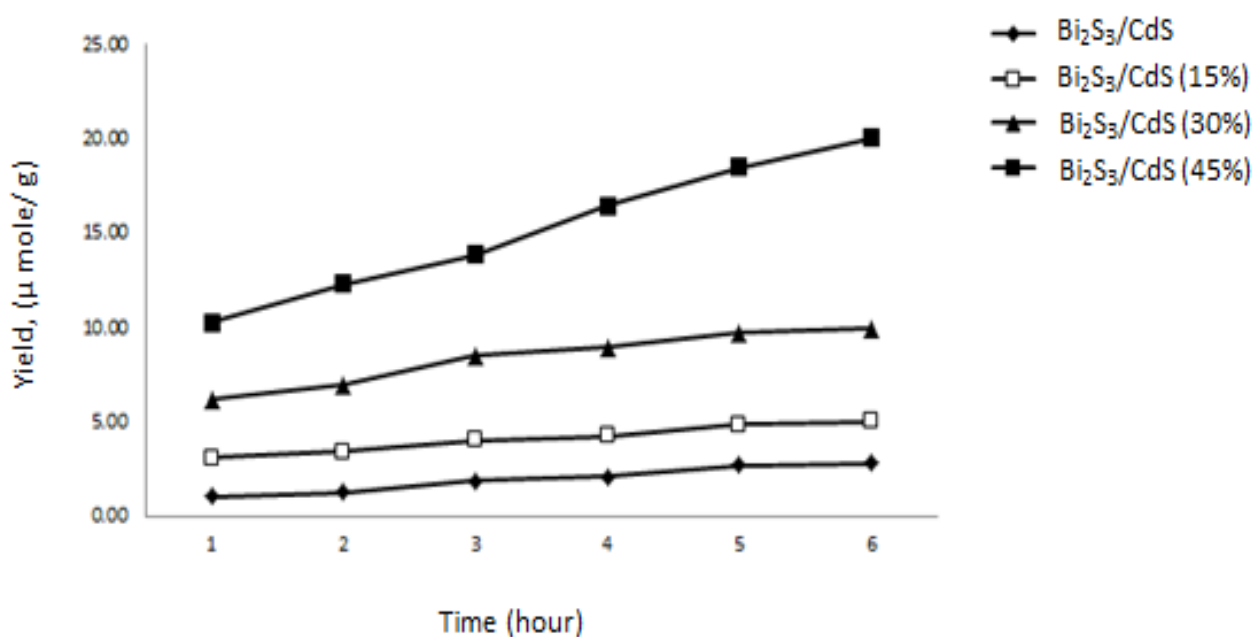


Figure 4-10 The yields of CH_3OH in the photocatalytic reduction of CO_2 with H_2O over various photocatalysts under visible light irradiation

The mechanism of photocatalytic reduction of CO_2 with H_2O to CH_3OH is shown in Figure 4.11. It can be seen from Figure 4 that both Bi_2S_3 and CdS can be used as photocatalyst for reducing CO_2 to CH_3OH under visible light. This is because the potentials of conduction bands of Bi_2S_3 and CdS are more negative than all those of methanol yield for. The detailed band structures are also pictured in Figure 4.11.

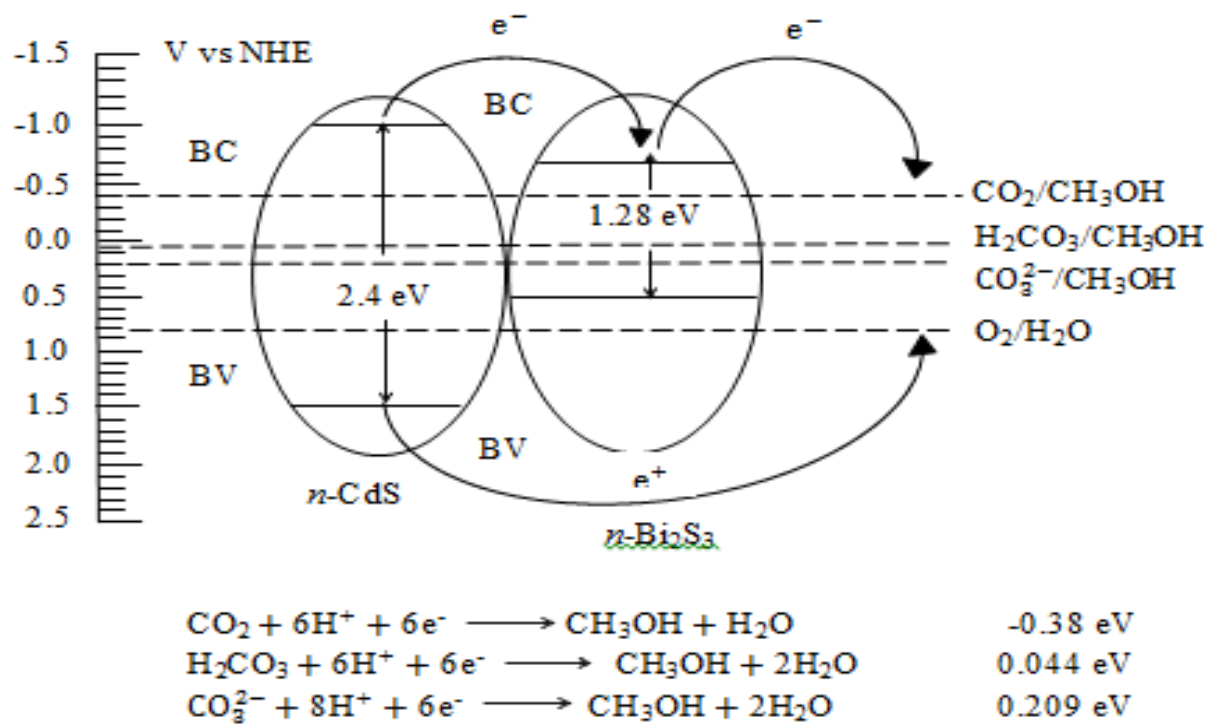


Figure 4-11 The mechanism of photocatalytic reduction for production of CH₃OH

5 CONCLUSION AND RECOMMENDATIONS

5.1 Conclusion

The Bi₂S₃/CdS photocatalyst were prepared by direct hydrothermal reactions between their corresponding salt and thio-urea. The Bi₂S₃/CdS photocatalyst was characterized by XRD. The modification of CdS with Bi₂S₃ can enhance its photocatalytic activity and visible light response. The highest yields of methanol over Bi₂S₃/CdS photocatalyst with 15%, 30% and 45% weight proportions under visible light irradiation were 5.04, 9.92 and 20.04 $\mu\text{mole/g}$, respectively.

5.2 Recommendations

Some recommendations to upgrade the effectiveness of this research had been identified through the whole experimental process of preparation and characterization of photocatalyst for the conversion of CO₂ to methanol which are:

- i) Wear personal protective equipment (PPE) such as gloves and goggles during the preparation of the catalyst since the chemicals used in the experiment are hazardous to health and irritant to eyes and skin.
- ii) The temperature of the hydrothermal autoclave should be constant so that the catalyst produced is at the same temperature range.
- iii) Use a ceramic mortar and pestle sets to reduce catalyst to very fine powders so that it can be produced larger amounts of methanol during photocatalytic activity.
- iv) Continue to bubble CO₂ so that the photocatalytic activity is continued to produce methanol.
- v) Monitor the temperature during the photocatalytic activity. The temperature range should be 30-35°C so that there is less loss of methanol to the air.

REFERENCES

- Aliwi S, Al-Jubori K F, 1989, *Sol Energy Mater*, 18(3-4), 223
- Anpo M, 1995, Approach to photocatalysis at the molecular level design of photocatalysts, detection of intermediate species and reaction mechanisms, *Solar Energy Materials and Solar Cells*; 38:221–38.
- Arakawa H, Aresta M, Armo J N, Barteau M A , Beckman E J, Bell A T, et al., 2001, Catalysis research of relevance to carbon management : progress, challenges, and opportunities, *Chemical Review*; 101 : 953–96.
- C. Song, 2006, Global challenges and strategies for control, conversion and utilization of CO₂ for sustainable development involving energy, catalysis, adsorption and chemical processing, *Catal. Today* 115, 2–32.
- Eggins B R, Robertson P K J, Murphy E P, Woods E, Irvine J T S, 1998, *J Photochem Photobiol A*, 118(1), 31
- Fujiwara H, Hosokawa H, Murakoshi K, Wada Y, Yanagida S, Okada T, Kobayashi H, 1997, *J Phys Chem B*, 101(41), 8270
- G.K. Mor, O.K. Varghese, M. Paulose, K. Shankar, C.A. Grimes, 2006, A review on highly ordered, vertically oriented TiO₂ nanotube arrays: fabrication, material properties, and solar energy applications, *Sol. Energy Mater. Sol. Cells* 90, 2011–2075.
- Ghoniem AF, 2011, Needs, resources and climate change : clean and efficient conversion technologies. *Progress in Energy and Combustion Science*; 37:15–51.
- Gill SS, Tsolakis A, Dearn KD, Rodríguez-Fernández J., 2010, Combustion characteristics and emissions of Fischer–Tropsch diesel fuels in IC engines. *Progress in Energy and Combustion Science*; 37:503–23.
- H.-C. Yang, H.-Y. Lin, Y.-S. Chien, J. Wu, H.-H. Wu, 2009, Mesoporous TiO₂/SBA-15, and Cu/TiO₂/SBA-15 composite photocatalysts for photoreduction of CO₂ to methanol, *Catal. Lett.* 131, 381–387.
- Hd Lasa, Serrano B, Salaices M. *Photocatalytic reaction engineering*, New York : Springer, 2005.
- Inoue T, Fujishima A, Konishi S, Honda K, 1979, *Nature*, 277(5698), 637
- J. Head, J. Turner, Analysis of the water-splitting capabilities of gallium indium phosphide nitride (GaInPN U.S. Department of Energy Journal of Undergraduate Research, January 2001, 26-31.

- J.M. Macak, H. Tsuchiya, A. Ghicov, K. Yasuda, R. Hahn, S. Bauer, P. Schmuki, 2007, TiO₂ nanotubes: self-organized electrochemical formation, properties and applications, *Curr. Opin. Solid State Mater. Sci.* 11, 3–18.
- K. Zhu, N.R. Neale, A. Miedaner, A.J. Frank, 2007, Enhanced charge-collection efficiencies and light scattering in dye-sensitized solar cells using oriented TiO₂ nanotubes arrays, *Nano Lett.* 7, 69–74.
- Kabra Kavita, Chaudhary Rubina, Sawhney R L, 2004, Treatment of hazardous organic and inorganic compounds through aqueous-phase photocatalysis: a review, *Industrial Engineering and Chemistry Research*, 43:7683–96.
- Li X, Chen J, Li H, Li J, Xu Y, Liu Y, Zhou J, 2011, Photoreduction of CO₂ to methanol over Bi₂S₃/CdS photocatalyst under visible light radiation, 413-417
- Li X, Chen X A, Li Z, 2012, *J Chem Eng Data*, 55(9), 3164
- Li X, Li H L, Huo S Q, Li Z, 2012, *Kinet Catal*, 51(5), 754
- Linsebigler A L, Lu G, Yates Jr. J T, 1995, Photocatalysis on TiO₂ surfaces : principles, mechanisms, and selected results, *Chemical Reviews*; 95:735–58.
- M. Hoffmann, S. Martin, W. Choi, D. Bahnemann, 1995, Environmental applications of semiconductor photocatalysis, *Chem. Rev.* 95, 69–96.
- Mori K, Yamashita H, Anpo M, 2012, Photocatalytic reduction of CO₂ with H₂O on various titanium oxide photocatalysts, *RSC Advance*; 2:3165.
- Muhammad Tahir, NorAishah Saidina Amin, 2013, Recycling of carbon dioxide to renewable fuels by photocatalysis: Prospects and challenges, *Renewable and Sustainable Energy Reviews* 25, 560–579
- S.C. Roy, O.K. Varghese, M. Paulose, C.A. Grimes, 2010, Toward solar fuels: Photocatalytic conversion of carbon dioxide to hydrocarbons, *ACS Nano* 4, 1259–1278.
- Vogel R, Hoyer P, Weller H, 1994, *J Phys Chem*, 98(12), 3183

APPENDIXES

APPENDIX A.1

A.1.1 Chemicals



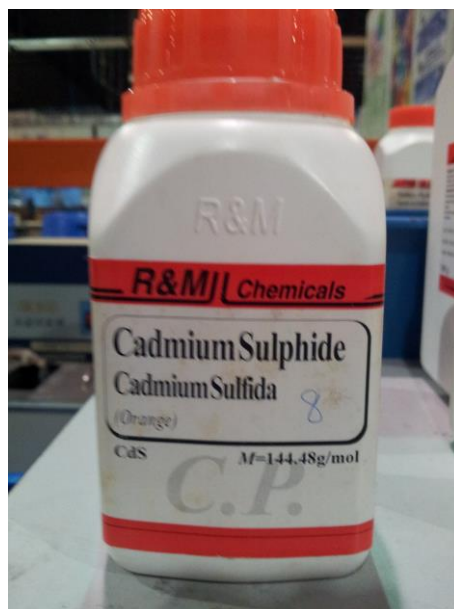
Bismuth (III) nitrate pentahydrate



Cadmium nitrate tetrahydrate



Thio-urea



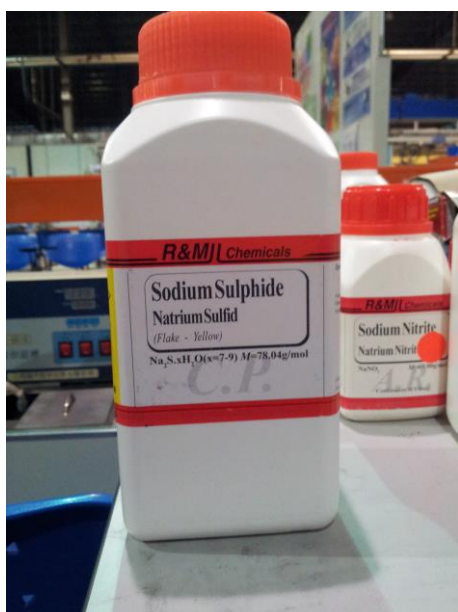
Cadmium sulphide



Sodium nitrite



Potassium hydroxide

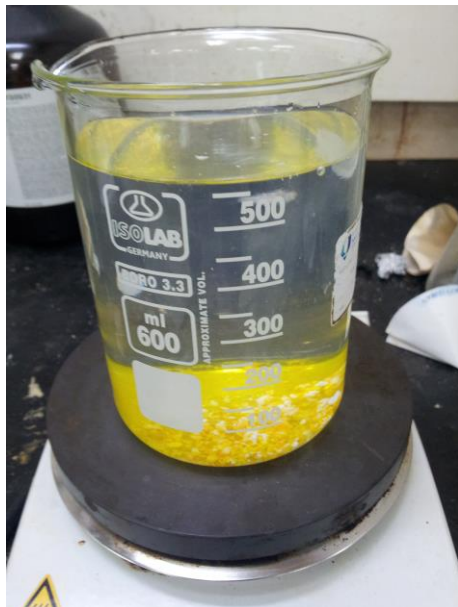


Sodium sulphide

A.1.2 Experiments

The pictures shown below are how the experiments were done.

A.1.2.1 Preparation of photocatalyst



Before the experiment start



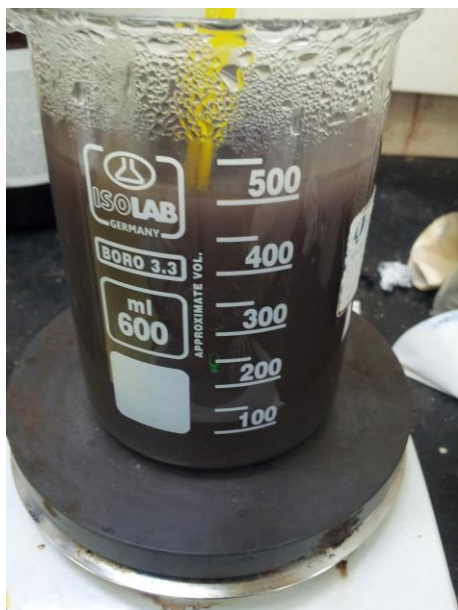
At the beginning of the experiment



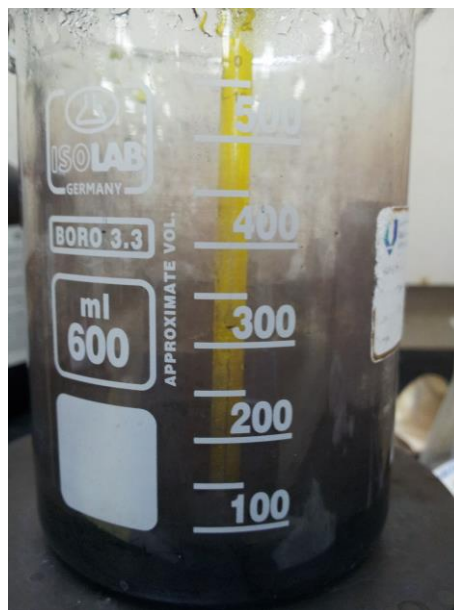
Time = 1 hour



Time = 2 hours



Time = 3 hours



Time = 6 hours



The catalyst after being dried in the oven for overnight

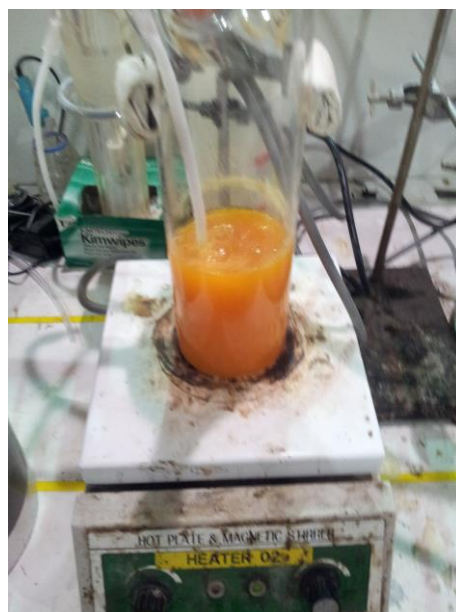
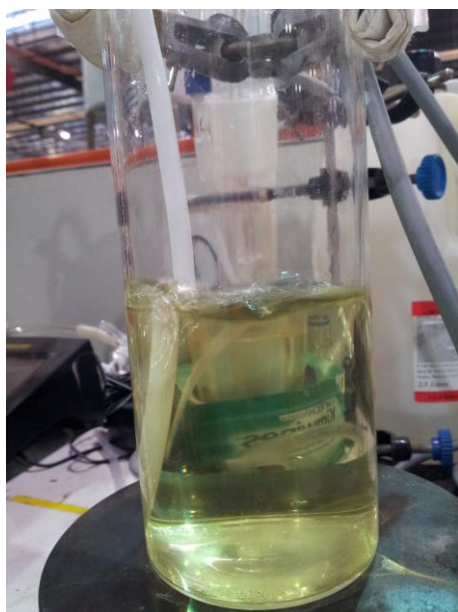
A.1.2.2 Photocatalytic reaction testing



The solution used in the reaction



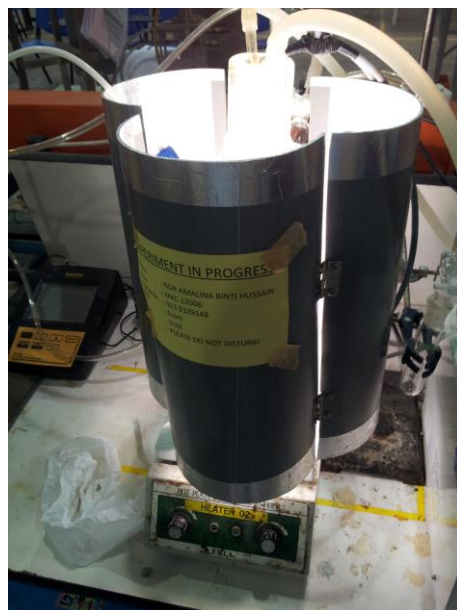
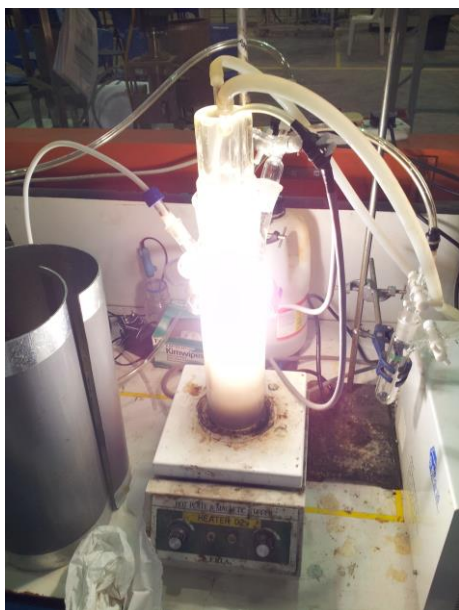
The set up of the reaction



CO₂ was bubbled through the solution in the reactor before irradiation for 30 minutes



0.2 g of catalyst powder was added into the solution



The irradiation lamp was turned on to start the photoreaction

A.1.3 Catalysts produced



$\text{Bi}_2\text{S}_3/\text{CdS}$ catalyst



$\text{Bi}_2\text{S}_3/\text{CdS}$ (15%) catalyst

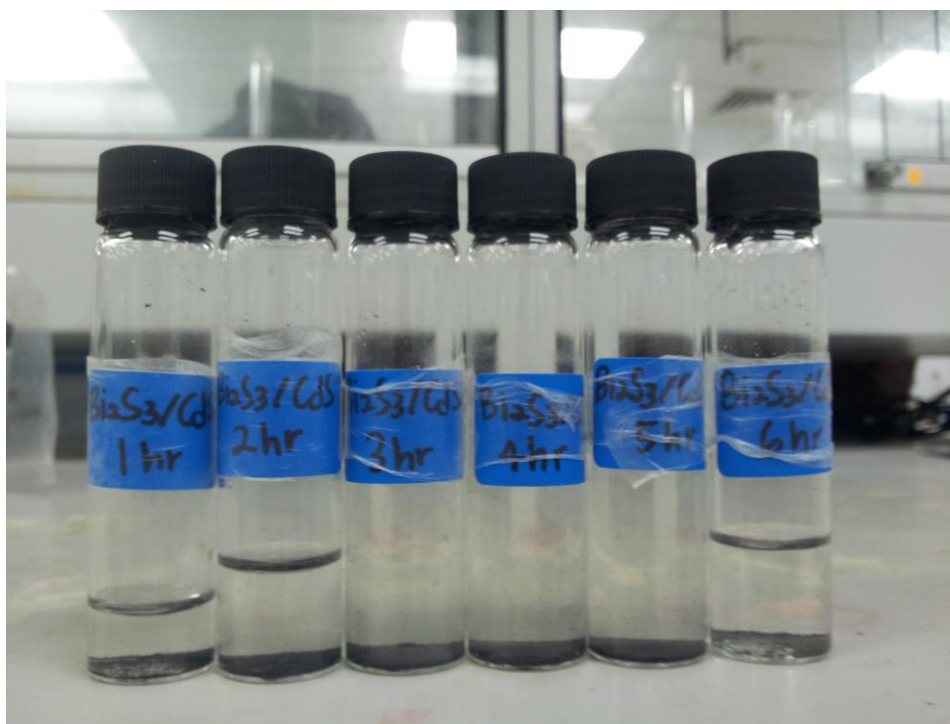


$\text{Bi}_2\text{S}_3/\text{CdS}$ (30%) catalyst

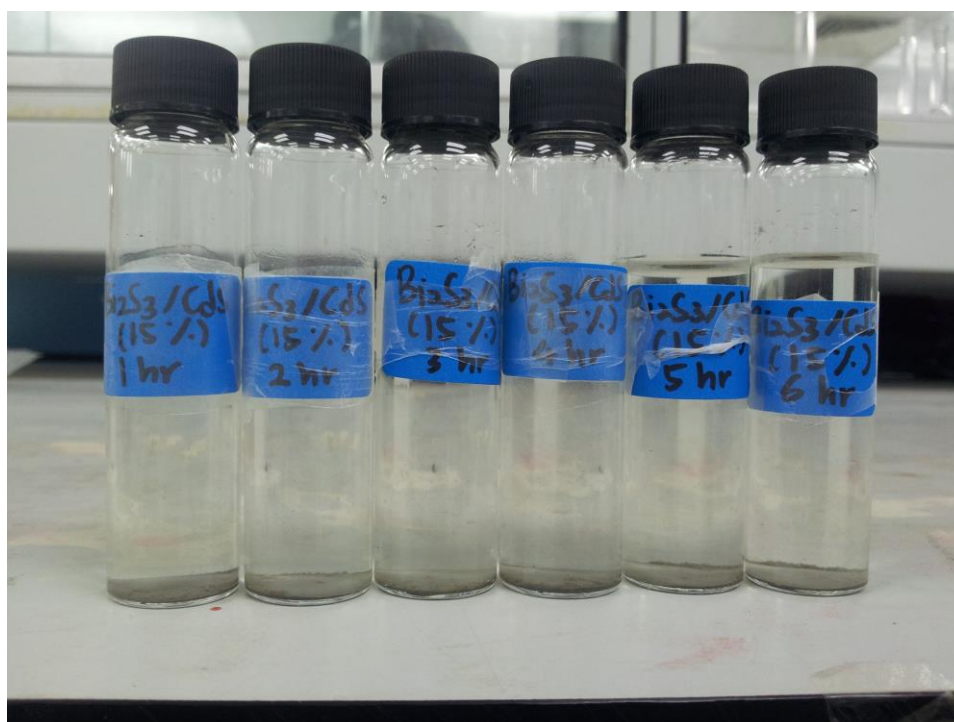


$\text{Bi}_2\text{S}_3/\text{CdS}$ (45%) catalyst

A.1.4 Products produced



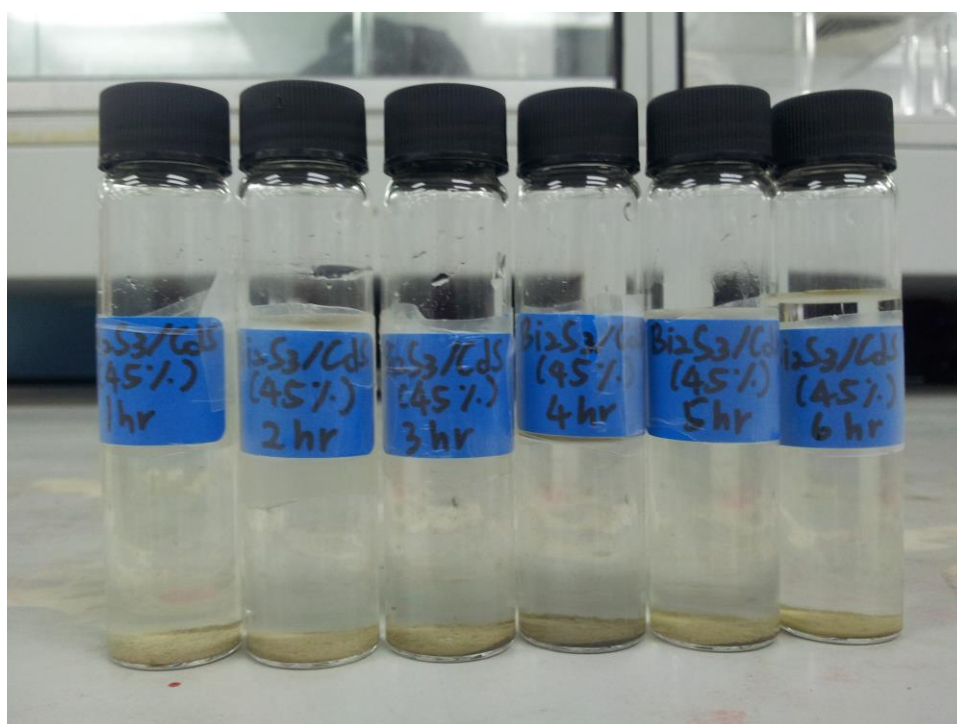
Using $\text{Bi}_2\text{S}_3/\text{CdS}$ catalyst (1-6 hours)



Using $\text{Bi}_2\text{S}_3/\text{CdS}$ (15%) catalyst (1-6 hours)



Using $\text{Bi}_2\text{S}_3/\text{CdS}$ (30%) catalyst (1-6 hours)



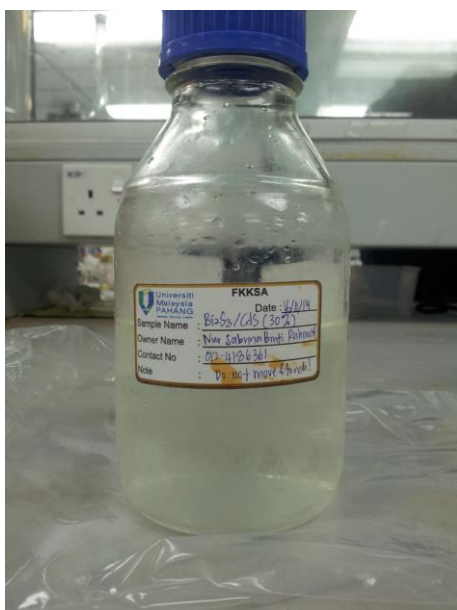
Using $\text{Bi}_2\text{S}_3/\text{CdS}$ (45%) catalyst (1-6 hours)



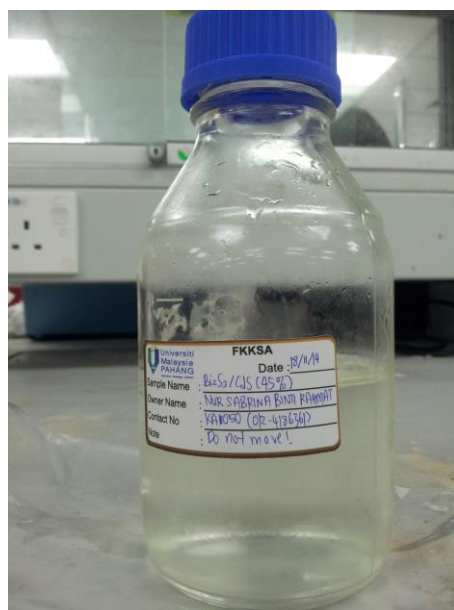
Using $\text{Bi}_2\text{S}_3/\text{CdS}$ catalyst



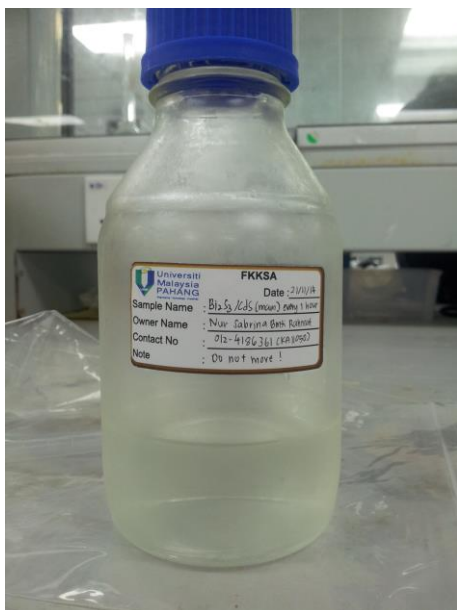
Using $\text{Bi}_2\text{S}_3/\text{CdS}$ (15%) catalyst



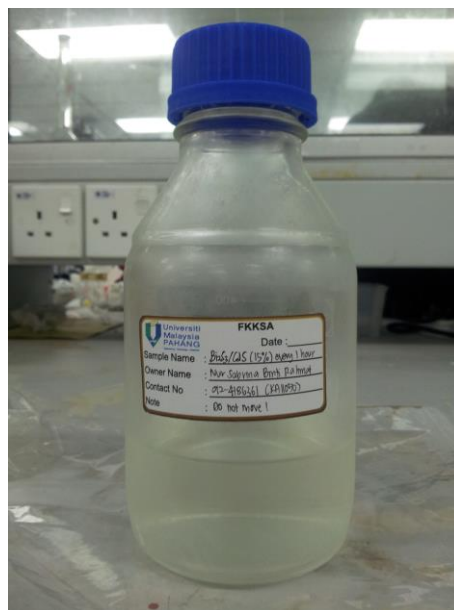
Using $\text{Bi}_2\text{S}_3/\text{CdS}$ (30%) catalyst



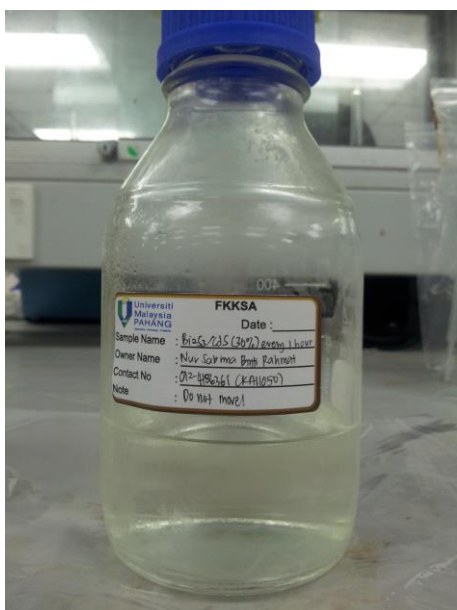
Using $\text{Bi}_2\text{S}_3/\text{CdS}$ (45%) catalyst



Using $\text{Bi}_2\text{S}_3/\text{CdS}$ catalyst (1-6 hours)



Using $\text{Bi}_2\text{S}_3/\text{CdS}$ (15)% catalyst (1-6 hours)



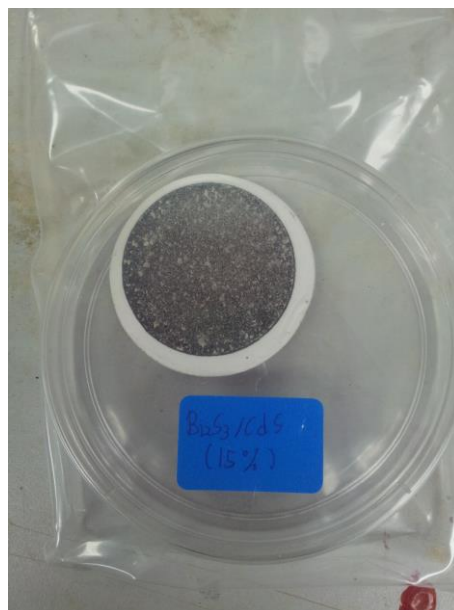
Using $\text{Bi}_2\text{S}_3/\text{CdS}$ (30)% catalyst (1-6 hours)



Using $\text{Bi}_2\text{S}_3/\text{CdS}$ (30)% catalyst (1-6 hours)



The precipitate of $\text{Bi}_2\text{S}_3/\text{CdS}$ catalyst filtered after photocatalytic reaction



The precipitate of $\text{Bi}_2\text{S}_3/\text{CdS}$ (15%) catalyst filtered after photocatalytic reaction



The precipitate of $\text{Bi}_2\text{S}_3/\text{CdS}$ (30%) catalyst filtered after photocatalytic reaction



The precipitate of $\text{Bi}_2\text{S}_3/\text{CdS}$ (45%) catalyst filtered after photocatalytic reaction



The precipitate of $\text{Bi}_2\text{S}_3/\text{CdS}$ catalyst (1-6 hours) filtered after photocatalytic reaction



The precipitate of $\text{Bi}_2\text{S}_3/\text{CdS}$ (15%) catalyst (1-6 hours) filtered after photocatalytic reaction



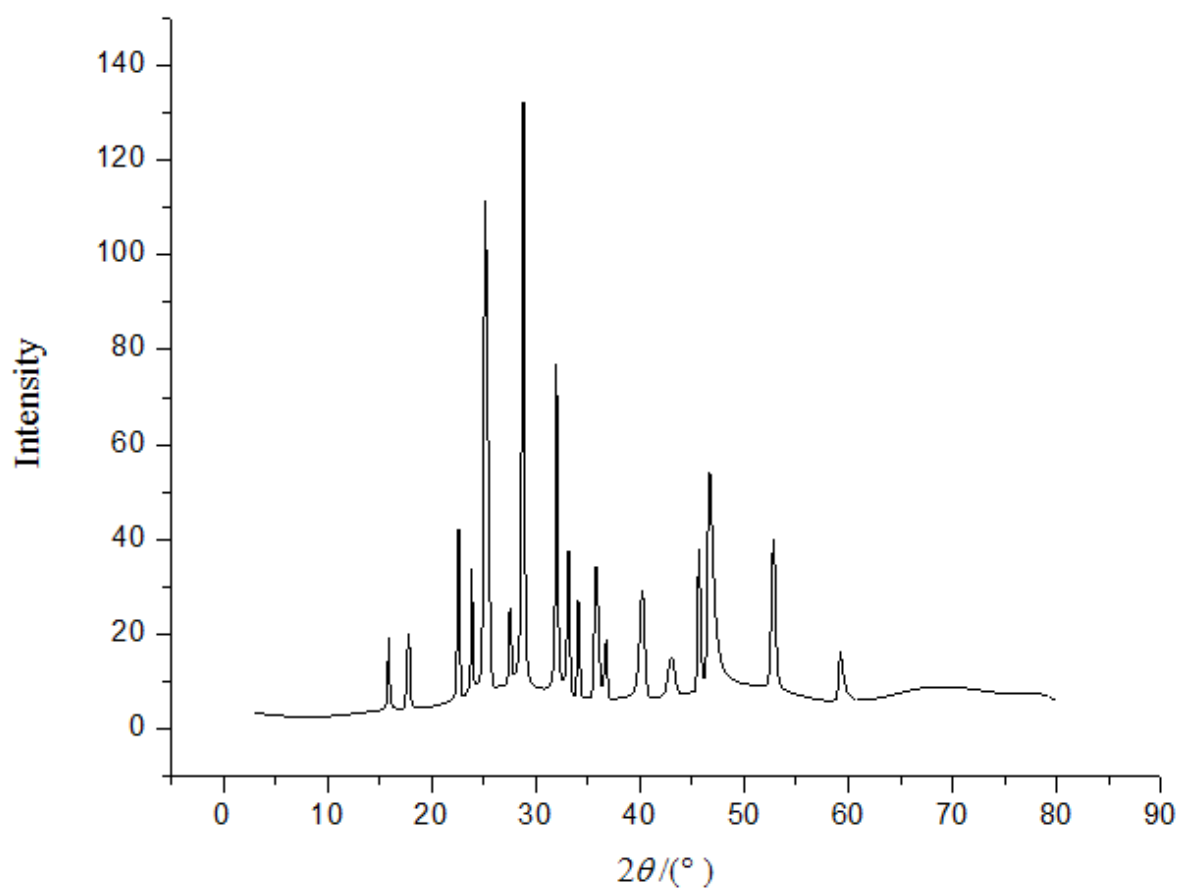
The precipitate of $\text{Bi}_2\text{S}_3/\text{CdS}$ (30%) catalyst (1-6 hours) filtered after photocatalytic reaction



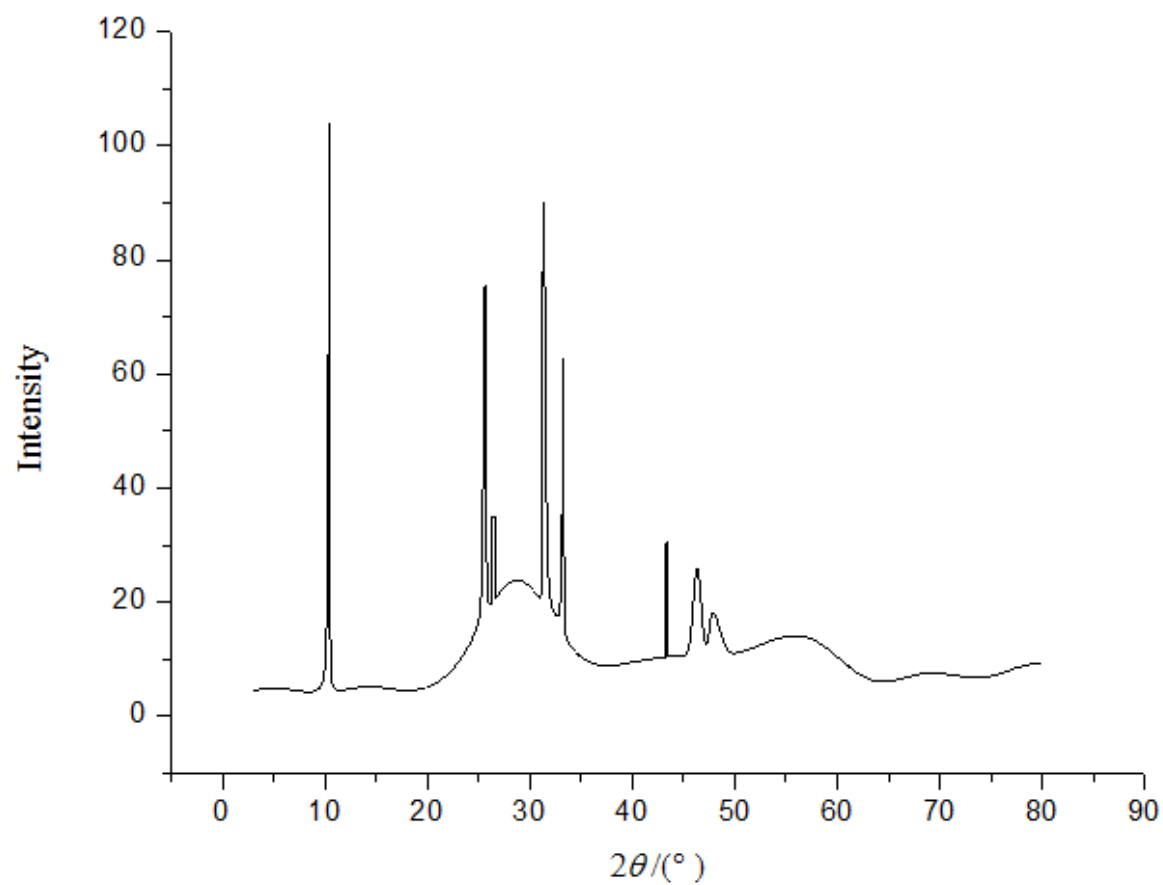
The precipitate of $\text{Bi}_2\text{S}_3/\text{CdS}$ (45%) catalyst (1-6 hours) filtered after photocatalytic reaction

A.1.5 XRD Analysis

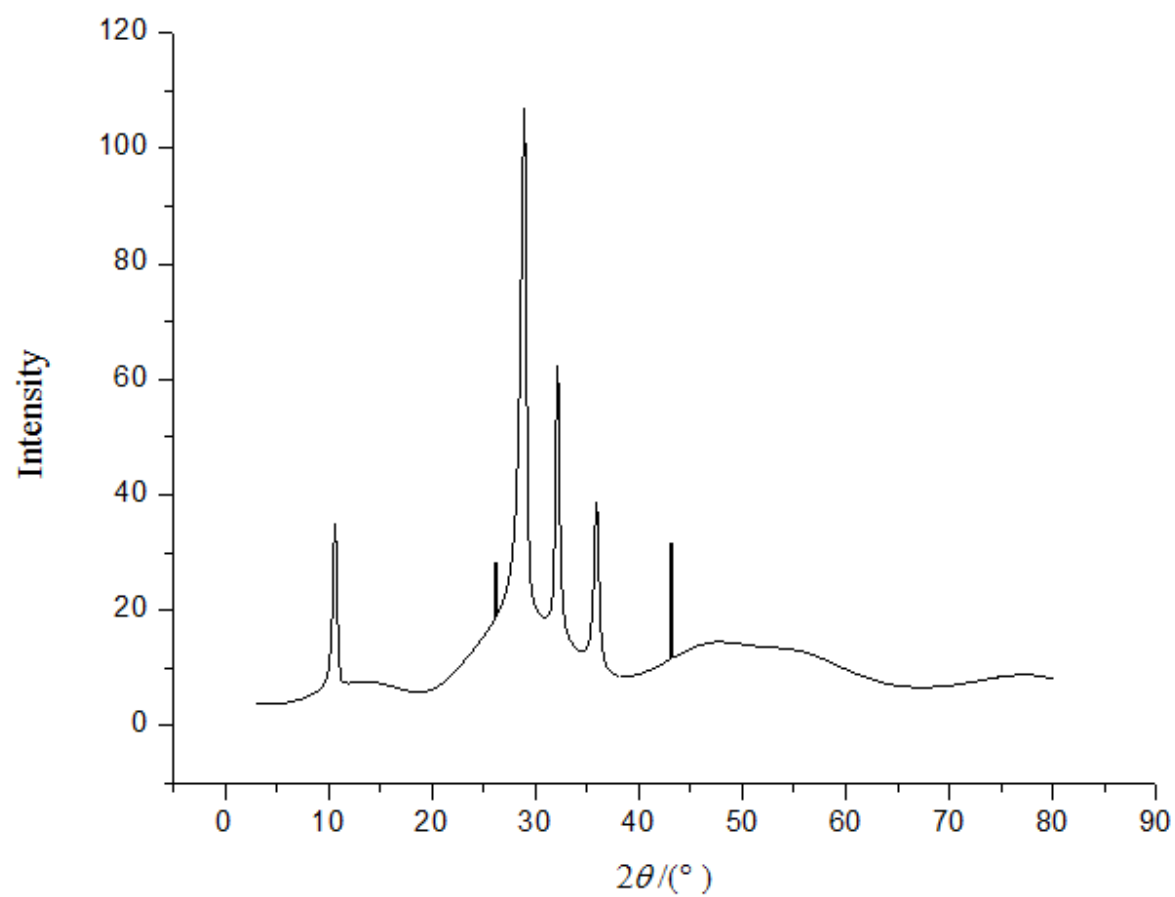
A.1.5.1 Bi₂S₃/CdS catalyst



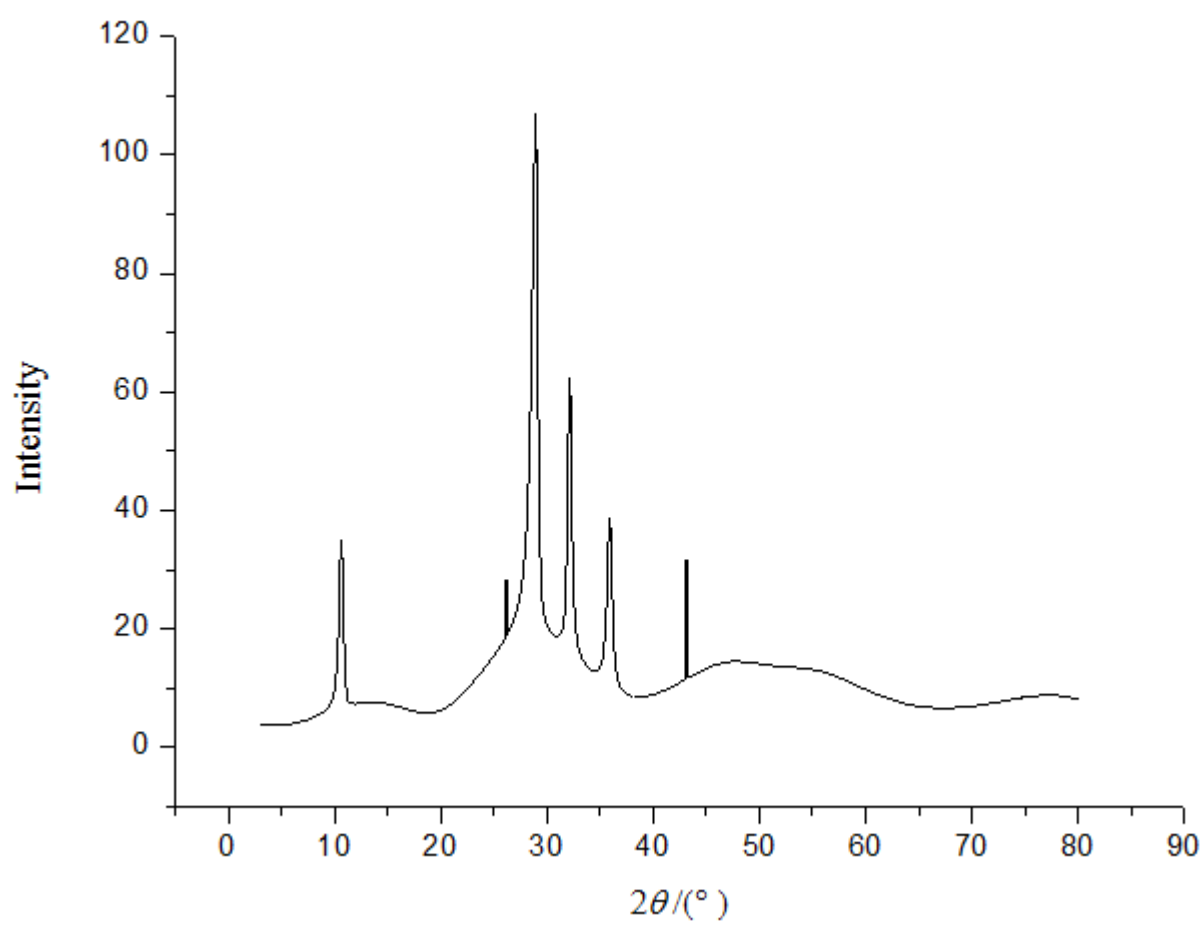
A.1.5.2 Bi₂S₃/CdS (15%) catalyst



A.1.5.3 Bi₂S₃/CdS (30%) catalyst

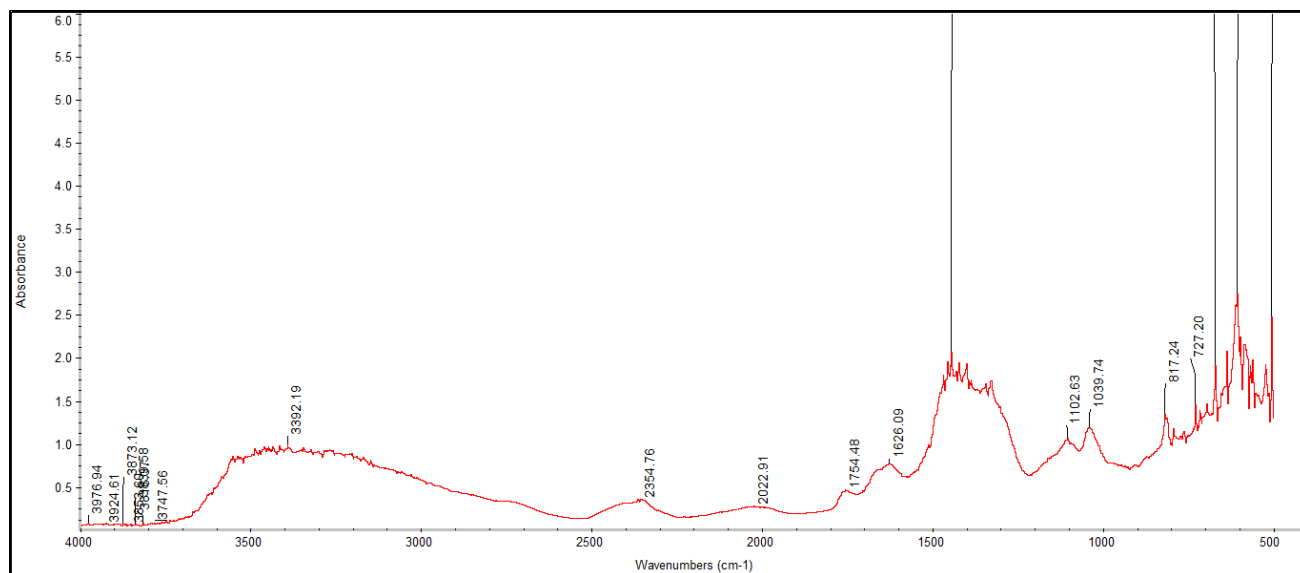


A.1.1.5.4 Bi₂S₃/CdS (45%) catalyst

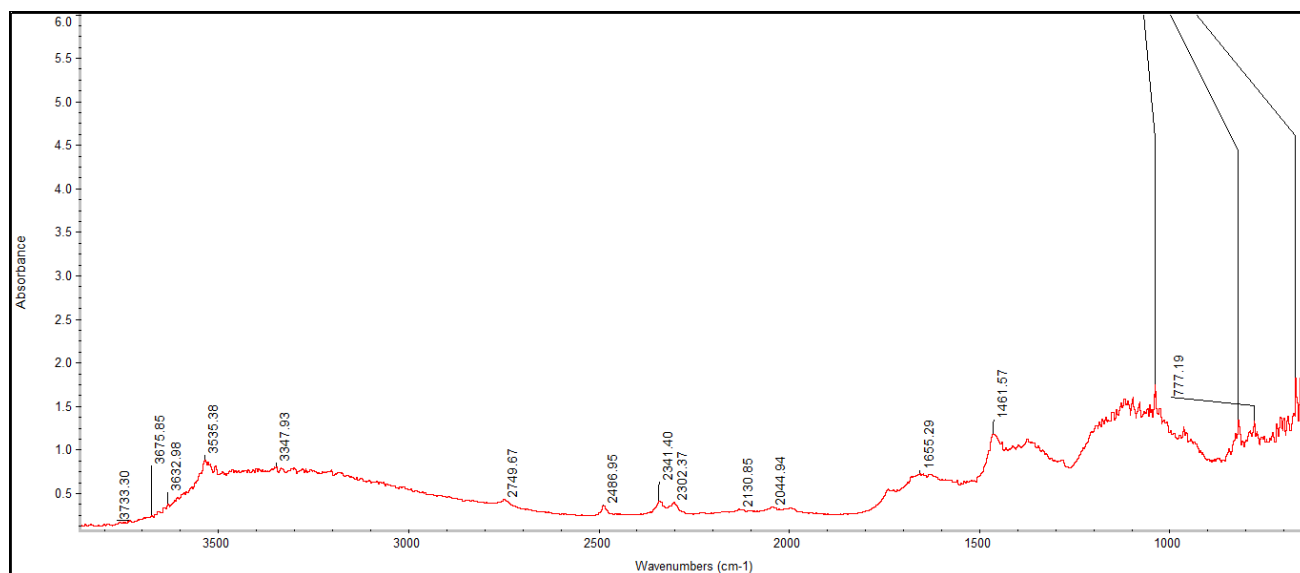


A.1.6 FTIR Analysis (Solid)

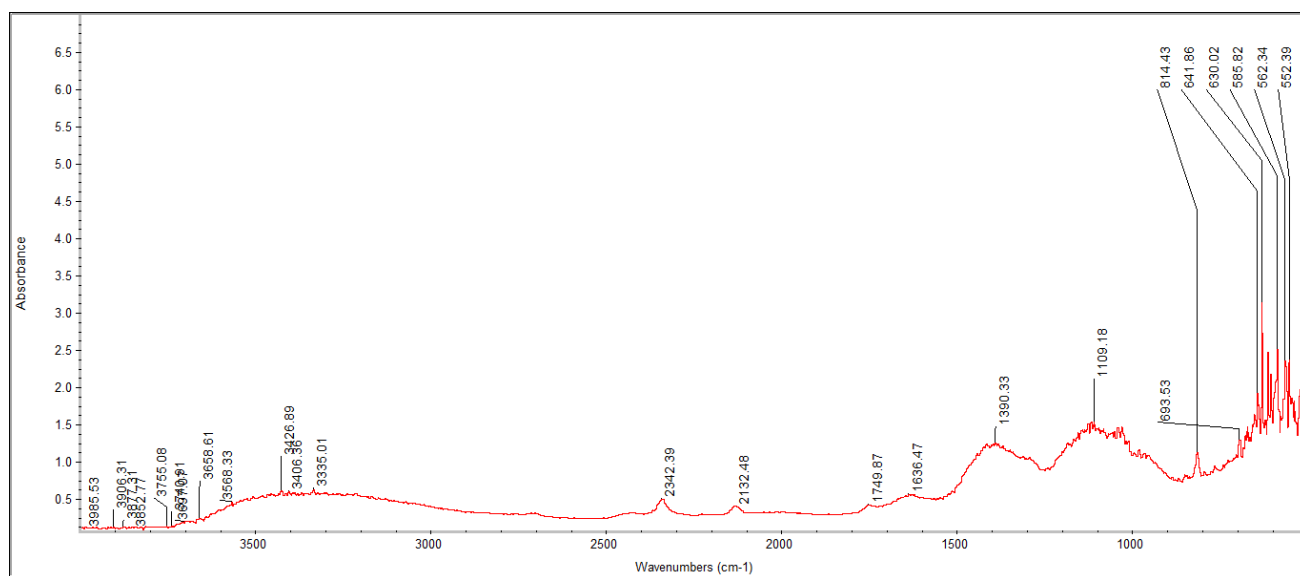
A.1.6.1 Bi₂S₃/CdS catalyst



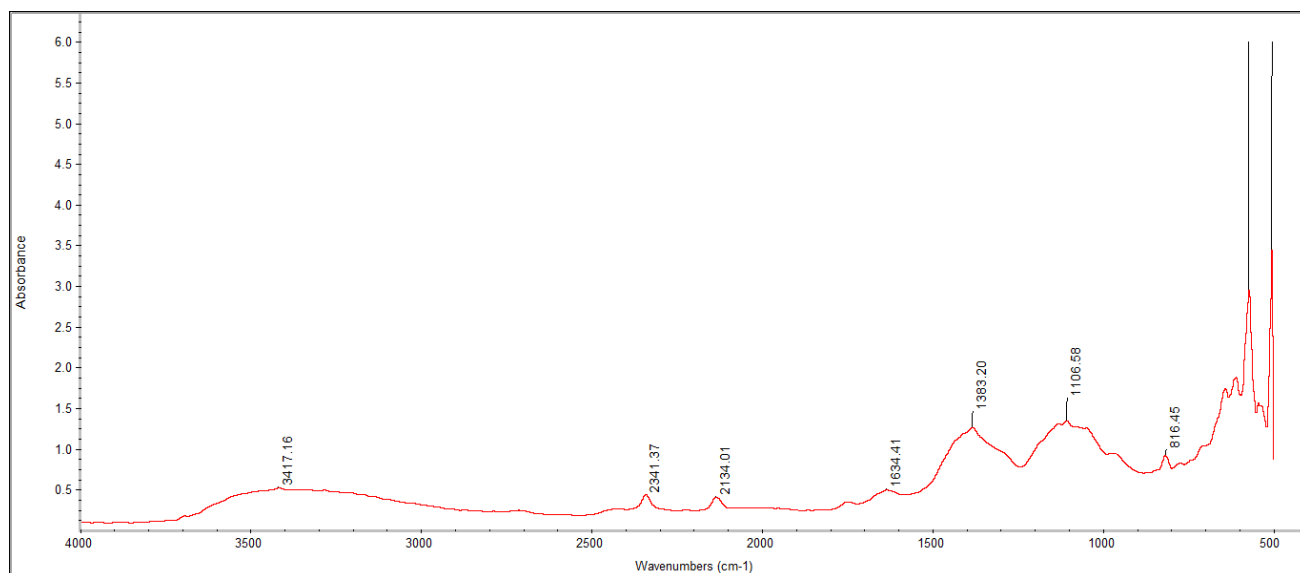
A.1.6.2 Bi₂S₃/CdS (15%) catalyst



A.1.6.3 Bi₂S₃/CdS (30%) catalyst

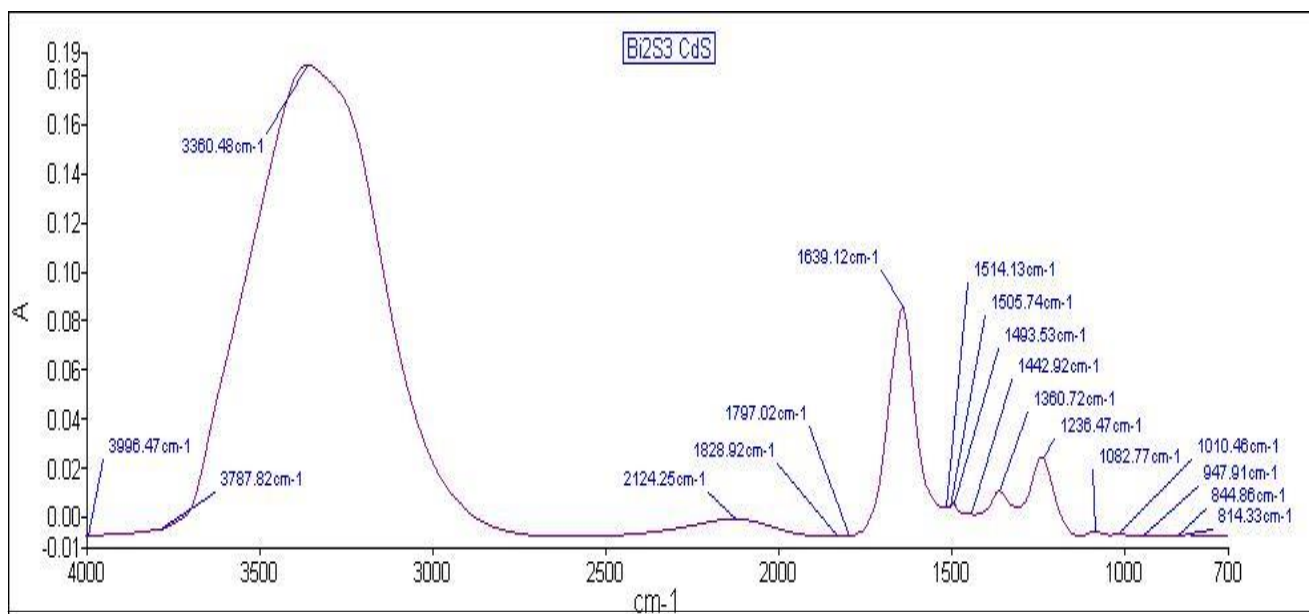


A.1.6.4 Bi₂S₃/CdS (45%) catalyst

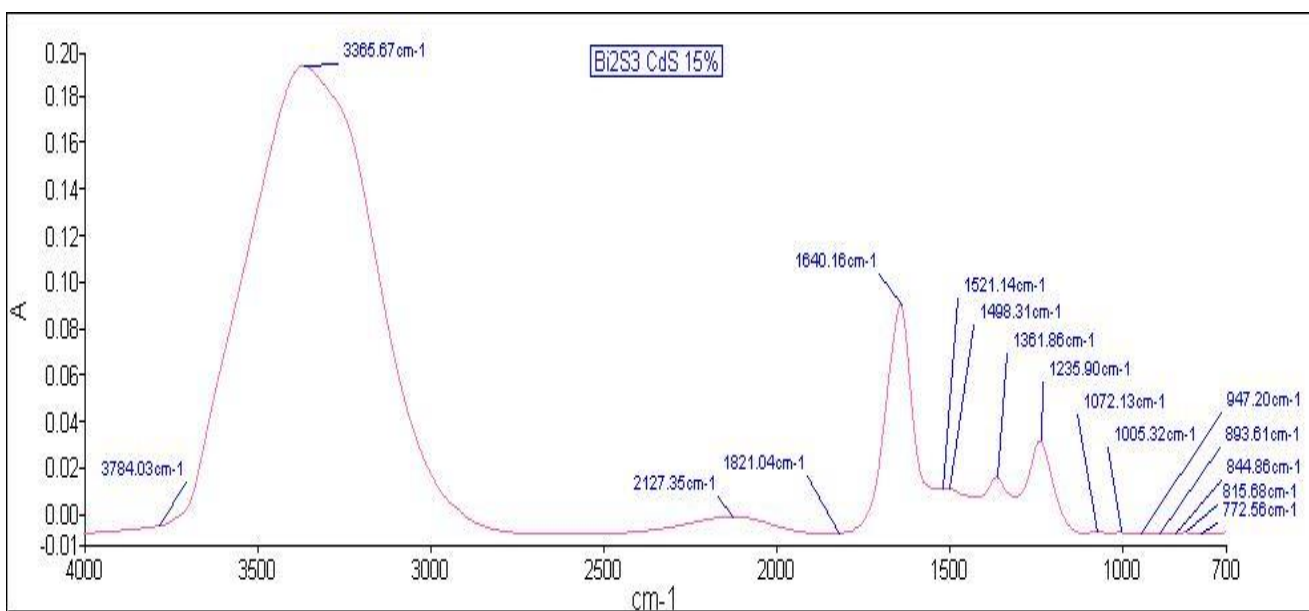


A.1.7 FTIR Analysis (Liquid)

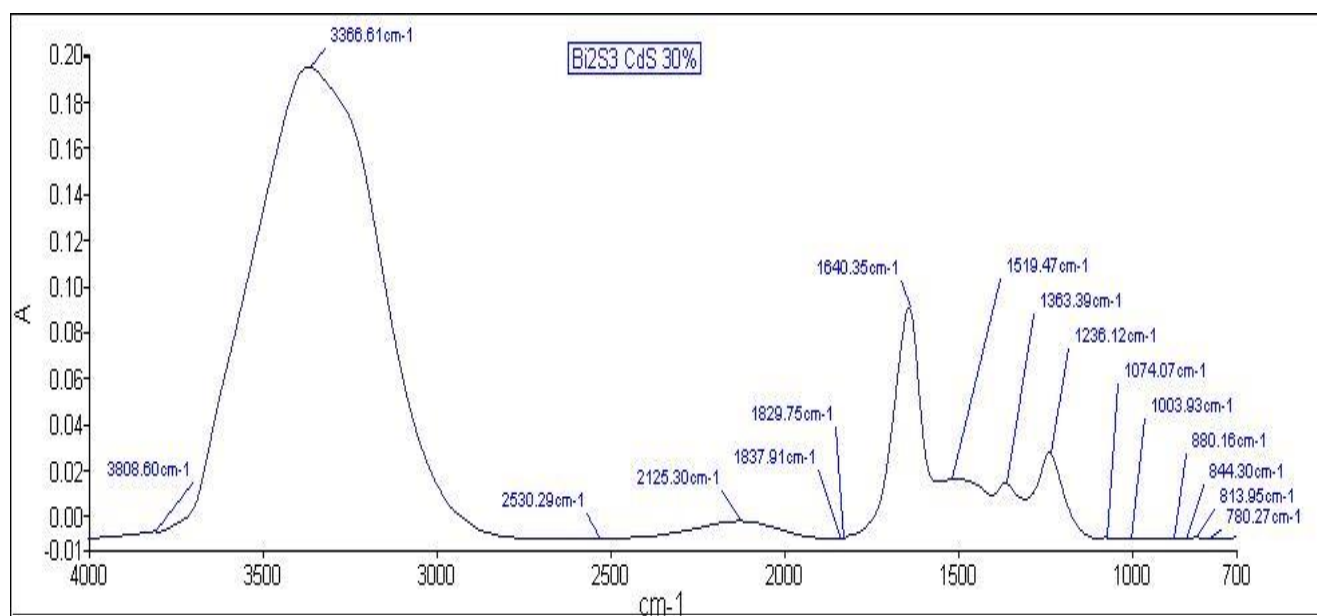
A.1.7.1 Bi₂S₃/CdS catalyst



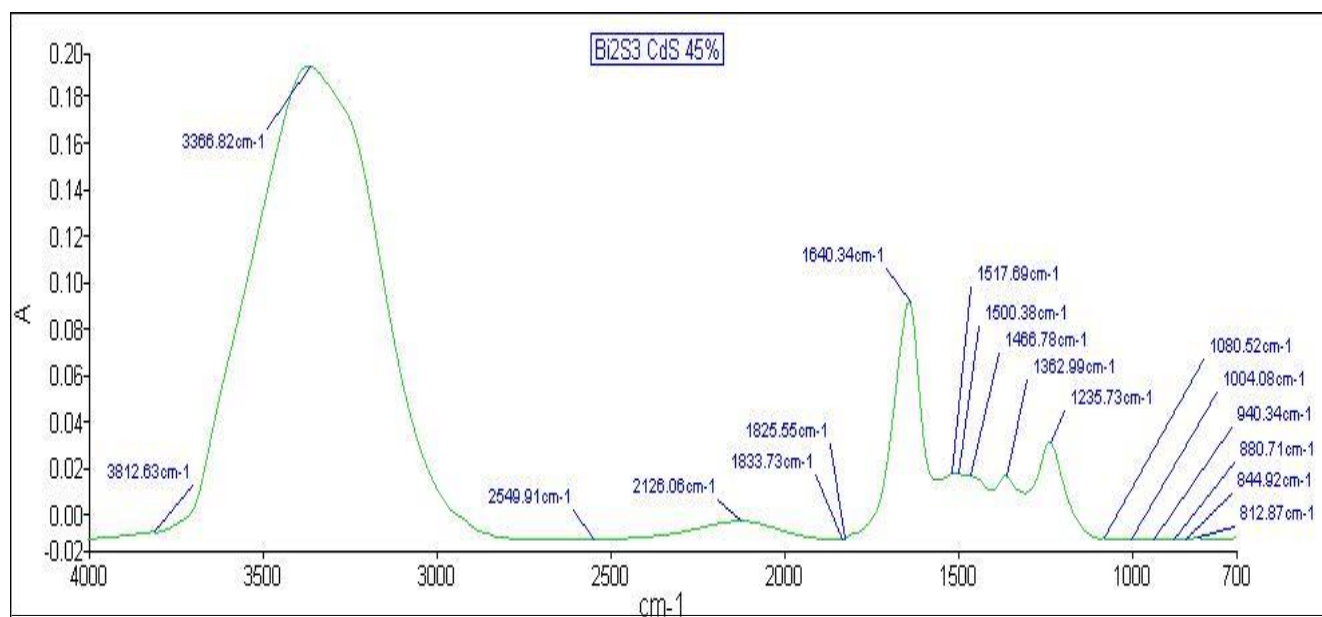
A.1.7.2 Bi₂S₃/CdS (15%) catalyst



A.1.7.3 Bi₂S₃/CdS (30%) catalyst



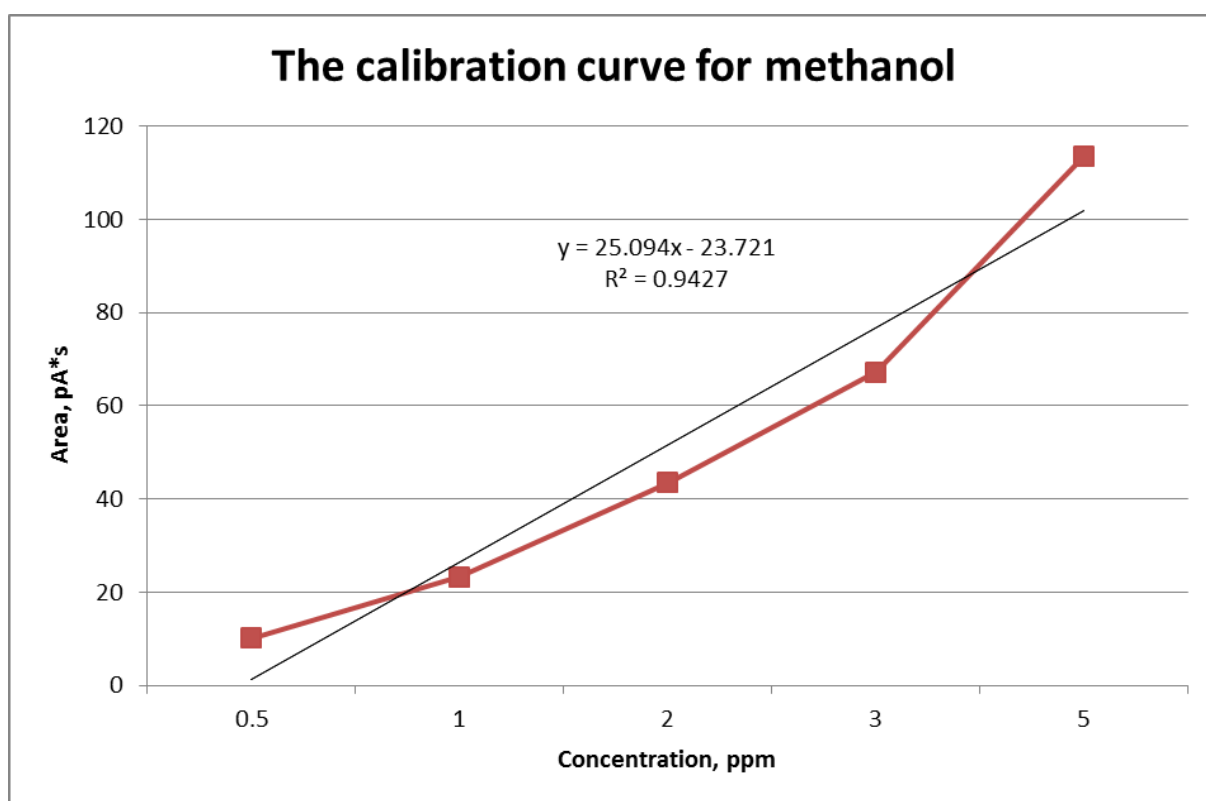
A.1.7.4 Bi₂S₃/CdS (45%) catalyst



A.1.8 GC-FID

A.1.8.1 Calibration curve

Ppm	Area
0.50	10.1125
1.00	23.3710
2.00	43.44089
3.00	67.22414
5.00	113.65617



A.1.8.2 Calculations in GC-FID

For the calculations, the formulas below are used :

$$\frac{\text{Area of sample}}{10.11247} \times 0.5 \text{ ppm} = a \text{ ppm} \quad (1)$$

$$\frac{a \text{ ppm} \times 10^{-3}}{32.04} = b \text{ } \mu\text{mole} \quad (2)$$

$$b \text{ } \mu\text{mole} \times 3.33 = c \text{ } \mu\text{mole/g} \quad (3)$$

Bi₂S₃/CdS catalyst

Time (hour)	Area (pA*s)	ppm	μ mole	μ mole/ g (catalyst)	μ mole/ g (catalyst)
1	0.2	0.009889	3.08639 x 10 ⁻⁷	1.02777 x 10 ⁻⁶	1.03
2	0.25	0.012361	3.85798 x 10 ⁻⁷	1.28471 x 10 ⁻⁶	1.28
3	0.37	0.018294	5.70981 x 10 ⁻⁷	1.90137 x 10 ⁻⁶	1.90
4	0.41	0.020272	6.32709 x 10 ⁻⁷	2.10692 x 10 ⁻⁶	2.11
5	0.53	0.026205	8.17892 x 10 ⁻⁷	2.72358 x 10 ⁻⁶	2.72
6	0.55	0.027194	8.48756 x 10 ⁻⁷	2.82636 x 10 ⁻⁶	2.83

Bi₂S₃/CdS (15%) catalyst

Time (hour)	Area (pA*s)	ppm	μ mole	μ mole/ g (catalyst)	μ mole/ g (catalyst)
1	0.6	0.029666	9.25916 x 10 ⁻⁷	3.0833 x 10 ⁻⁶	3.08
2	0.67	0.033127	1.03394 x 10 ⁻⁶	3.44302 x 10 ⁻⁶	3.44
3	0.78	0.038566	1.20369 x 10 ⁻⁶	4.00829 x 10 ⁻⁶	4.01
4	0.83	0.041038	1.28085 x 10 ⁻⁶	4.26523 x 10 ⁻⁶	4.27
5	0.95	0.046972	1.46603 x 10 ⁻⁶	4.88189 x 10 ⁻⁶	4.88
6	0.98	0.048455	1.51233 x 10 ⁻⁶	5.03606 x 10 ⁻⁶	5.04

Bi₂S₃/CdS (30%) catalyst

Time (hour)	Area (pA*s)	ppm	μ mole	μ mole/ g (catalyst)	μ mole/ g (catalyst)
1	1.2	0.059333	1.85183×10^{-6}	6.1666×10^{-6}	6.17
2	1.35	0.066749	2.08331×10^{-6}	6.93742×10^{-6}	6.94
3	1.65	0.081582	2.54627×10^{-6}	8.47907×10^{-6}	8.48
4	1.74	0.086032	2.68516×10^{-6}	8.94157×10^{-6}	8.94
5	1.89	0.093449	2.91663×10^{-6}	9.71239×10^{-6}	9.71
6	1.93	0.095427	2.97836×10^{-6}	9.91795×10^{-6}	9.92

Bi₂S₃/CdS (45%) catalyst

Time (hour)	Area (pA*s)	ppm	μ mole	μ mole/ g (catalyst)	μ mole/ g (catalyst)
1	2	0.098888	3.08639×10^{-6}	1.02777×10^{-5}	10.28
2	2.4	0.118665	3.70366×10^{-6}	1.23332×10^{-5}	12.33
3	2.7	0.133499	4.16662×10^{-6}	1.38748×10^{-5}	13.87
4	3.2	0.15822	4.93822×10^{-6}	1.64443×10^{-5}	16.44
5	3.6	0.177998	5.55549×10^{-6}	1.84998×10^{-5}	18.50
6	3.9	0.192831	6.01845×10^{-6}	2.00414×10^{-5}	20.04